Kingdom of Saudi Arabia
Imam Mohammad bin Saud Islamic
University College of Science
Chemistry Department

Influence of V_2O_5 dopant-dose on the efficiency of $AlMgO_4$ performance in eliminating basic fuchsin and indigo carmine dyes from polluted water.

Research submitted as partial fulfillment requirements for the completion of the BSc Degree in Chemistry

By

Adulrahman Mushabab Ali Abu Shatat (441017619)
&

Faisal bader Abdullah albilali (440014762)

&

Saad Khalid Saad Alotaibi (441016744)

Supervisor

Dr. Faisal Khuwayshan Algethami

February - 2024

Acknowledgement & Dedication

We express our heartfelt gratitude to our supervisor, Dr. Faisal Algethami, for his exceptional guidance and efficient administration. Furthermore, we would like to extend our appreciation to the outstanding scholars in the Department of Chemistry at Imam Muhammad bin Saud University's College of Science for their steadfast commitment and essential mentorship. This research is devoted to our families as a token of appreciation for their steadfast support and encouragement.

Figures		
Fig. No.	**Caption**	**Page No.**
1	**The contact time trend of INC sorption onto the $MgAl_2O_4$ nanocomposite.**	**20**
2	**The contact time trend of INC sorption onto the 2.5%V2O5@$MgAl_2O_4$ nanocomposite.**	**20**
3	**The contact time trend of INC sorption onto the 5%V2O5@$MgAl_2O_4$ nanocomposite.**	**21**
4	**The contact time trend of INC sorption onto the 10%V2O5@$MgAl_2O_4$ nanocomposite.**	**21**
5	**The contact time trend of BFC sorption onto the $MgAl_2O_4$ nanocomposite.**	**22**
6	**The contact time trend of BFC sorption onto the 2.5%V2O5@$MgAl_2O_4$ nanocomposite.**	**22**
7	**The contact time trend of BFC sorption onto the 5%V2O5@$MgAl_2O_4$ nanocomposite.**	**23**
8	**The contact time trend of BFC sorption onto the 10%V2O5@$MgAl_2O_4$ nanocomposite.**	**23**
9	**The PF investigation of INC sorption onto $MgAl_2O_4$ composite.**	**25**
10	**The PF investigation of INC sorption onto 2.5%V2O5@$MgAl_2O_4$ composite.**	**25**
11	**The PF investigation of INC sorption onto 5%V2O5@$MgAl_2O_4$ composite.**	**26**
12	**The PF investigation of INC sorption onto 10%V2O5@$MgAl_2O_4$ composite.**	**26**
13	**The PF investigation of BFC sorption onto $MgAl_2O_4$ composite.**	**27**
14	**The PF investigation of BFC sorption onto 2.5%V2O5@$MgAl_2O_4$ composite.**	**27**
15	**The PF investigation of BFC sorption onto 5%V2O5@$MgAl_2O_4$ composite.**	**28**
16	**The PF investigation of BFC sorption onto 10%V2O5@$MgAl_2O_4$ composite.**	**28**
17	**The PS investigation of INC sorption onto $MgAl_2O_4$ composite.**	**29**
18	**The PS investigation of INC sorption onto 2.5%V2O5@$MgAl_2O_4$ composite.**	**29**

Abstract

This work employed a rapid technique for the synthesis of $MgAl_2O_4$, 2.5%V_2O_5@$MgAl_2O_4$, 5%V_2O_5@$MgAl_2O_4$, and 10%V_2O_5@$MgAl_2O_4$ composites. The produced composites were examined for their ability to adsorb INC and BFC from water. The $MgAl_2O_4$, 2.5%V_2O_5@$MgAl_2O_4$, 5%V_2O_5@$MgAl_2O_4$, and 10%V_2O_5@$MgAl_2O_4$ exhibited q_t values of 75.91, 108.37, 147.30, and 118.54 mg g^{-1}, respectively, for INC. For BFC, the q_t values were 154.27, 167.38, 198.65, and 173.85 mg g^{-1}, respectively. The equilibrium of INC sorption was achieved after 90 minutes, but BFC sorption equilibration onto the four sorbents only required 60 minutes. The kinetics of the adsorption process were analyzed using PF and PS models. The data demonstrates that the sorption of INC removals on four sorbents adhered to the rate-order model. In addition, the analysis of the BFC rate showed that BFC sorption onto $MgAl_2O_4$ and 2.5%V_2O_5@$MgAl_2O_4$ agreed with the PF, whereas its sorption onto 5%V_2O_5@$MgAl_2O_4$ and 10%V_2O_5@$MgAl_2O_4$ conformed to the PS. In addition, the rate-control output of INC removal demonstrated that the LFD regulated the sorption on 5%V_2O_5@$MgAl_2O_4$ and 10%V_2O_5@$MgAl_2O_4$, while IPD regulated it on $MgAl_2O_4$ and 2.5% V_2O_5@$MgAl_2O_4$. Regarding the BFC outputs, it was found that IPD had influence over the sorption of BFC onto all sorbents except for $MgAl_2O_4$.

الملخص باللغة العربية

استخدمت هذهر الدراسة طريقة سريعة لتخليق مركبات MgAl2O4 و 2.5%V2O5@MgAl2O4 و 5%V2O5@MgAl2O4, 10%V2O5@MgAl2O4. تمت دراسة قدرة المركبات المنتجة على امتزاز صبغتى BFC,INC من الماء. أظهرت$MgAl_2O_4$ ، $2.5\%V_2O_5@MgAl_2O_4$، و$5\%V_2O_5@MgAl_2O_4$، و $10\%V_2O_5@MgAl_2O_4$ قدرة امتزاز تبلغ 75.91، و108.37، و147.30، و118.54 ملجم/ جرام، على التوالي بالنسبة لـ .INC وبالنسبة لـBFC ، كانت قدرة الامتزاز 154.27، 167.38، 198.65، و173.85 ملجم/جرام على التوالي. وصل امتزاز INC بعد 90 دقيقة، لكن موازنة امتصاص BFC على المواد الماصة الأربعة لم تتطلب سوى 60 دقيقة. تم تحليل حركية عملية الامتزاز باستخدام نماذج PF وPS . توضح النتائج أن عمليات إزالة INC على الأربعة مواد المحضرة يتبع نموذج ترتيب المعدل PS. بالإضافة إلى ذلك، اتضح ان معدل سرعة الامتزاز أن لـــ BFCعلى $MgAl_2O_4$ و $\%V_2O_5@MgAl_2O_4$ يتوافق مع PF، في حين أن امتزازها على $5\%V_2O_5@MgAl_2O_4$ و $10\%V_2O_5@MgAl_2O_4$ يتوافق مع PS . بالإضافة إلى ذلك، أظهر ناتج التحكم في معدل إزالة INC أن LFD يتحكم في امتزازها على $5\%V_2O_5@MgAl_2O_4$ و$10\%V_2O_5@MgAl_2O_4$، بينما ينظمه IPD على $MgAl_2O_4$ و $2.5\%V2O5@MgAl_2O_4$ فيما يتعلق بمخرجاتBFC ، وجد أن IPD كان المتحكم في امتزاز BFC على جميع المواد المازة باستثناء $MgAl_2O_4$.

Chapter One

Introduction and Literature Review

1. Introduction

1.1. Nanomaterial

Nanoscale materials are substances with a dimension of 100 nm or less [1]. Because of their wide applications, several methods have been employed for synthesizing nanomaterials, broadly categorized as bottom-up approaches involving assembling atoms or molecules to form bigger structures within the nanoscale regime. The second perspective can be characterized as a top-down approach, wherein the size of bulk materials is diminished to the nanoscale [4-6]. From these two main routes, numerous methodologies have been created. Still, the main ones are Solvothermal, sol-gel, and Green methodologies. Solvothermal is one of the most environmentally friendly and promising synthesis methods. The solvothermal approach uses solvents to optimize particle size distribution and shape control. This technique homogenizes metal salts and adjusts the medium pH to alkaline with a basic solution. The target nanomaterial controls the homogenized solution's thermal treatment temperature and time [7]. The sol-gel process is the most used method for creating nanomaterials. A reaction between precursors happens in a suitable solvent where a surfactant or nonaqueous solvent controls the particle size [8]. In green nanomaterial manufacturing, capping substrates might be plant extracts or microorganisms. Biosynthesis of nanomaterials from seeds, leaves, stems, roots, and latex. Green technology was the safest approach to making nanoparticles. Scientists use bacteria, algae, fungi, and plants to make cheap, energy-efficient, and

environmentally friendly metal nanoparticles. Green synthetic methods are replacing physicochemical ones in the industry [9, 10]. Zinc oxide (ZnO) nanoparticles have wide applications in various fields. According to recent research, Alumina nanoparticles are one of the most popular nanosized materials in the United States. It is now in first or second place among nanoscale materials sales in the United States [11]. Many different technologies have found use for nanoscale ZnO, including adsorption, photocatalysis, lithium batteries, coating, rocket fuel, gelled fuel, ceramics, and solar cells [12]. Additionally, ZnO was believed to improve the anti-cancer effects of immunotherapy that uses a tumor cell vaccination [13]. Due to its low specific gravity, strength, and stiffness, MgO has many potential uses. These include but are not limited to, biosensors, computers, electronics, vehicles, aircraft, adsorbents, catalysts, superconducting products, and batteries [14]. Leilei et al., prepared NiO-MgO-Al_2O_3 nanocomposite using absolute ethanol as a solvent. The mixed ion solution was acidified by nitric acid, and the final mixture was covered and stirred at room temperature for 5.0 h. Lastly, the mixture was transferred to a petri dish, protected, and put into a 60 ◦C drying oven for 48 h. The resulting gel was calcined at 600 ◦C for 5.0 h [15]. Yi et al., prepared NiO-MgO-Al_2O_3 by the wet impregnation method starting with commercial spherical Al_2O_3. $Mg(NO_3)_2$ was dissolved in water; after adding Al2O3, the mixture was kept at room temperature for 8.0 hours. The product was filtered from the mixture, dried at 110 °C for 24.0 h, and calcined at 500°C for 5.0 h. The collected material after

calcination was added to Ni solution and kept at room temperature for 8.0 h. The solid was filtered, dried at 110°C overnight, and then calcined at 500°C for 5.0 h [16]. Hayder et al. prepared MgO composite using a hot plate stirrer set to 60°C to continuously mix 100 ml of deionized water with aluminum nitrate and calcium nitrate until the salts dissolve. Ammonium hydroxide (NH4OH) was gradually added with constant stirring until a gel formed, dried, and calcined for 2 hours at 550°C [17]. Electronics, magnetism, biology, medicines, cosmetics, the environment, catalysis, and materials are just some of the many applications for nanoscale materials. The promising future of nanotechnology has led to a rise in funding for its study and development around the world. Research into, and investment in, nanotechnology has increased dramatically since 1999 [18]. The use of nanomaterials in water purification is one of their significant implications. To put it simply, water contamination is any change, whether physical or chemical, in water quality that has an adverse effect on living organisms or renders water unfit for critical uses. It has far-reaching consequences on people, families, and communities. Water pollution poses a serious threat to life on Earth because water is essential for all life forms [19]. There are many different ways to define water contamination due to the wide range of causes and consequences it might have. Basically, it lowers the standard of water, which causes problems for aquatic life and makes it less effective as a resource. Rivers, oceans, lakes, rains, wells, and groundwater are all at risk, as are fish and other aquatic life, and the economic value of the water can decrease

as a result. The result of water pollution is that it makes water unsafe for human, animal, plant, and aquatic life consumption [20]. Collecting groundwater through prospecting, drilling, or springs is crucial to the river's flow [21]. Over the past few years, a scarcity of clean water for human and agricultural usage has resulted from the alarming rise in water pollution. Waterborne disease epidemics have been commonplace since the spread of polluted water systems [22]. Land-based human activities, such as manufacturing and garbage disposal, primarily contribute to ocean pollution [23].

1.2 Water treatment methods

To guarantee that residents can access potable water, public and wastewater systems use various water treatment methods:

1.2.1. Heating

Parasites and bacteria, both of which are invisible to the naked eye but can be lethal, may be present in water from a variety of sources and distribution systems. Once the water has boiled, cover it and let it cool before drinking [24].

1.2.2. Filtration

Regarding chemical and physical processes, filtration is one of the most reliable options for purifying water. Large-scale chemicals and microscopic contaminants are removed from the air thanks to filtration. Because filtering does not entirely remove mineral salts, filtered water is preferable to unfiltered water for health reasons [25].

1.2.3. Ozonation

Water purification by ozonation includes adding the powerful oxidant ozone to the water supply. Ozone, or triatomic oxygen, is a highly reactive gas that may destroy many chemicals and bacteria. Water purification and destroying organic and pollutant compounds are two of the many benefits of ozone treatment, an enhanced oxidation process [26].

1.2.4. Ion Exchange

Chemical and environmental engineers have used the ion exchange (IX) technique for years. Initially, its primary usage was in water softening, which removes calcium and magnesium ions from water at the treatment plant or as a point-of-use treatment procedure [27].

1.2.5. Chemical Precipitation

The chemical precipitation of heavy metals from wastewater is a standard treatment method. Removal of impurities from water using precipitating agents (coagulants) such as ferrous or aluminum sulfates by altering the pH, electro-oxidizing potential, or coprecipitation [28].

Taking in Water (1.3.7)

Adsorption is the phenomenon whereby chemicals move from one phase to another, whether between liquid and solid, gas and liquid, or gas and solid. Intermolecular forces are effective at removing contaminants from wastewater. Adsorption can have either a physical or chemical form. Reversible physisorption occurs in the presence of weak physical forces like van der Waals.

This adsorption type occurs at or near the adsorbate's critical temperature. Chemisorption, on the other hand, involves the adsorbate and solid surface forming a chemical connection. However, it always exists as a single layer, and the adsorbates are easily removed by washing. Both processes are possible simultaneously or as needed. Surface area, adsorbate type and beginning concentration, solution pH, temperature, competing chemicals, and adsorbent nature and dose are all important variables to consider when studying adsorption processes [29, 30].

1.3. Aim of the study

This study aimed to prepare $MgAl_2O_4$, $2.5\%V_2O_5@MgAl_2O_4$, $5\%V_2O_5@MgAl_2O_4$, and $10\%V_2O_5@MgAl_2O_4$ triple composite as environmentally safe sorbents. A one-put route was adopted inorder to simplify the process. The study create prepared double and triple composites will tested for removing organic pollutants exampled by indigo caramine (INC) and basic fuchsin (BFC), and their sorption kinetics would be investigated.

Chapter Two

Materials and Methods

2. Materials and methods

2.1 Materials

Indigo caramine (INC), basic fuchsin (BFC), and Ammonium metavanidate ($(NH_4)_2VO_3$) were provided by Fluka, USA. Magnesium chloride-6-hydrate 99% ($MgCl_2$-$6H_2O$) and D(+)-Glucose monohydrate (GL) were provided from Riedel-de-Haen, Germany. Aluminum chloride hexahydrate 97% ($AlCl_3$-$6H_2O$) was purchased from (LOBA CHEMIE, Mumbai, India).

2.2. Preparation of $MgAl_2O_4$ and its V_2O_5 composites

11.46 g of $AlCl_3$-$6H_2O$, 24.6 g of $MgCl_2$-$6H_2O$, and 10 g of GL were transferred to a 500 mL beaker. About 15 mL of distilled water was added. The mixture was turned into a clear solution by heating on a hotplate (120°C), then the hotplate temperature was raised (250°C) until the GL was carbonized. The obtained powder was grinned, transferred to a porcelain dish, and calcined at 600°C for 3.0 h. The process was repeated using the typical Al-Mg amounts with the addition of a proper amount of $(NH_4)_2VO_3$to obtain 2.5%V_2O_5@$MgAl_2O_4$, 5% V_2O_5@$MgAl_2O_4$, and 10% V_2O_5@$MgAl_2O_4$.

2.3. Preparation of INC and BFC solutions

0.1g of INC was weighed using an analytical balance and transferred to a 1L volumetric flask to obtain 100 mg L^{-1} INC solution. Then, 600 mL of DW was added to the flask and put into an ultrasonic path. The resulting solution was completed to the neck mark by DW. The 100 mg L^{-1} BFC solution was prepared similarly to INC.

2.4. Adsorption

0.05g of each sorbent ($MgAl_2O_4$, 2.5% V_2O_5@$MgAl_2O_4$, 5% V_2O_5@$MgAl_2O_4$, and 10% V_2O_5@$MgAl_2O_4$) was measured in a separate 150 mL beaker. 100 mL of the 100 mg L^{-1} INC solution was poured into each beaker. A portion of the mixture was withdrawn till the INC sorption reached the equilibrium. The aliquots were filtered via a 0.22μm syringe filter, and the absorbance was measured utilizing a UV-Vis-spectrophotometer (λ_{max} = 610 nm). Also, the BFC adsorption (λ_{max} = 510 nm) was studied similarly to INC.

Chapter Three

Results and Discussion

3. Results and discussion

3.1. Contact time study

The contact time study of INC and BFC sorption onto the as-prepared $MgAl_2O_4$, 2.5%V2O5@$MgAl_2O_4$, 5%V2O5@$MgAl_2O_4$, and 10%V2O5@$MgAl_2O_4$ were studied. The INC and BFC absorbance measured during the study were employed for calculating their remaining concentrations (unadsorbed) at each time interval via Eq. 1. Using Eq. 2 was utilized to calculate the adsorption capacity at each period (the INC or BFC milligrams adsorbed onto one gram of sorbent, q_t, mg g^{-1}).

$$C_t = \frac{Absorbance_{sample}}{Absorbance_{standard}} \times conc._{standard} \quad (1)$$

$$q_t = \frac{(C_o - C_t)\,V}{m}, \quad (2)$$

Fig. 1, 2, 3, and 4 demonstrate the adsorption trend of INC onto $MgAl_2O_4$, 2.5%V2O5@$MgAl_2O_4$, 5%V2O5@$MgAl_2O_4$, and 10%V2O5@$MgAl_2O_4$, respectively, while Fig. 5, 6, 7, and 8 demonstrated the BFC sorption trend of INC onto the same four sorbents, respectively. The $MgAl_2O_4$, 2.5%V2O5@$MgAl_2O_4$, 5%V2O5@$MgAl_2O_4$, and 10%V2O5@$MgAl_2O_4$ showed q_t values for INC were 75.91, 108.37, 147.30 and 118.54 mg g^{-1}, respectively, while for BFC they showed q_t values of 154.27, 167.38, 198.65 and 173.85 mg g^{-1}, respectively. The INC sorption reached its equilibrium at 90 minutes, while 60 minutes was sufficient for BFC sorption equilibration onto the four sorbents.

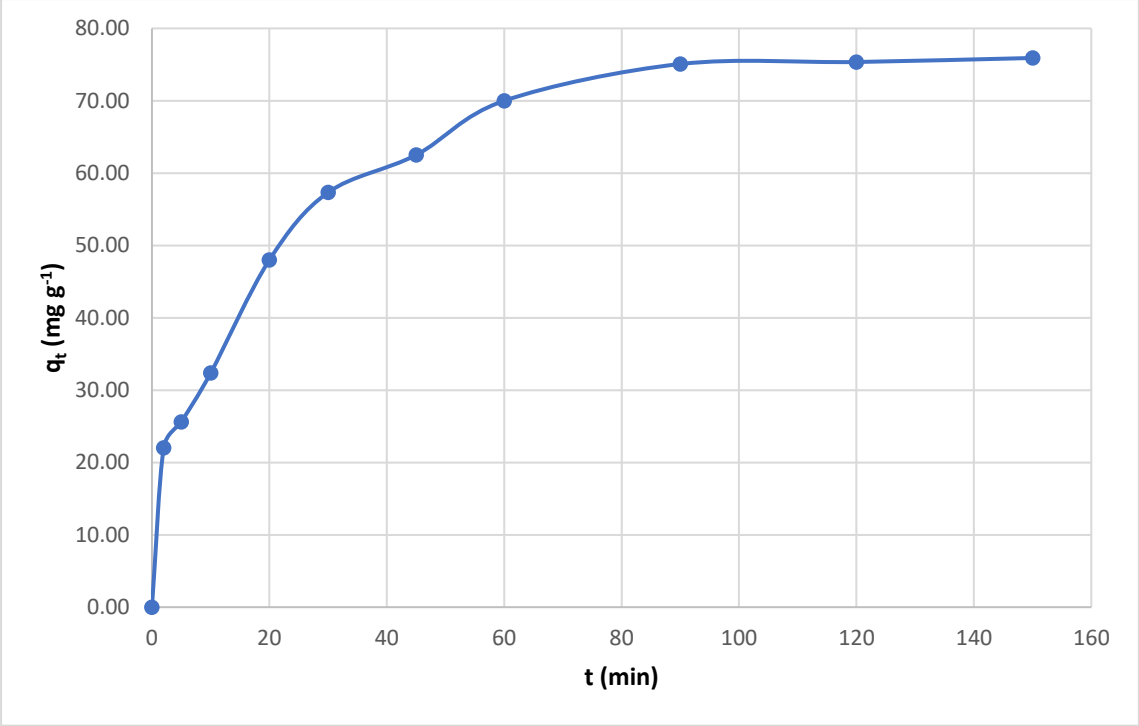

Fig. 1 The contact time trend of INC sorption onto the $MgAl_2O_4$ nanocomposite.

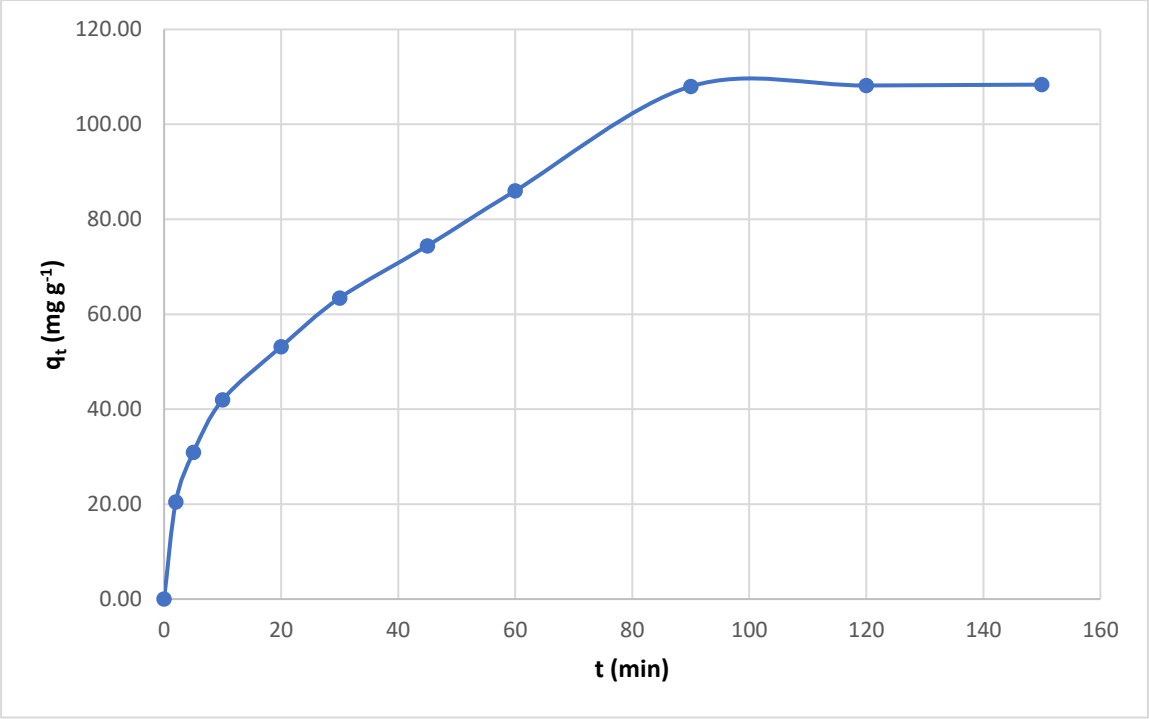

Fig. 2 The contact time trend of INC sorption onto the 2.5%V_2O_5@$MgAl_2O_4$ composite.

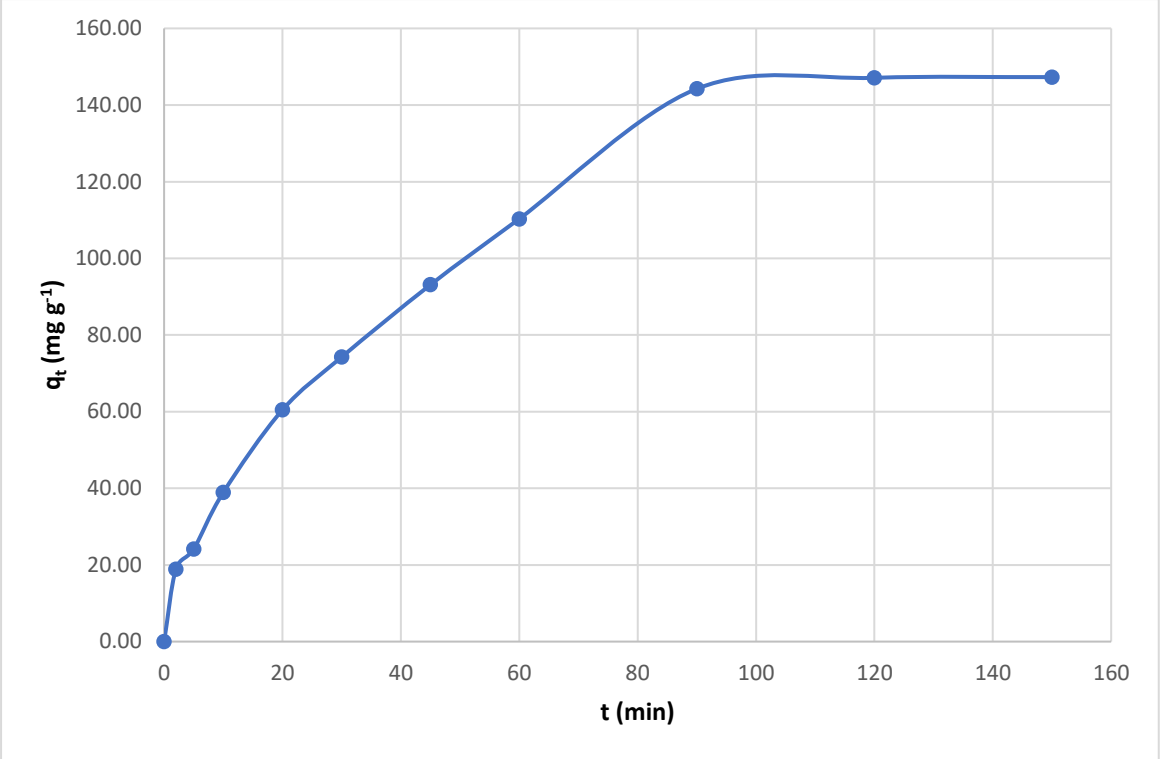

Fig. 3 The contact time trend of INC sorption onto the 5%V_2O_5@$MgAl_2O_4$ composite.

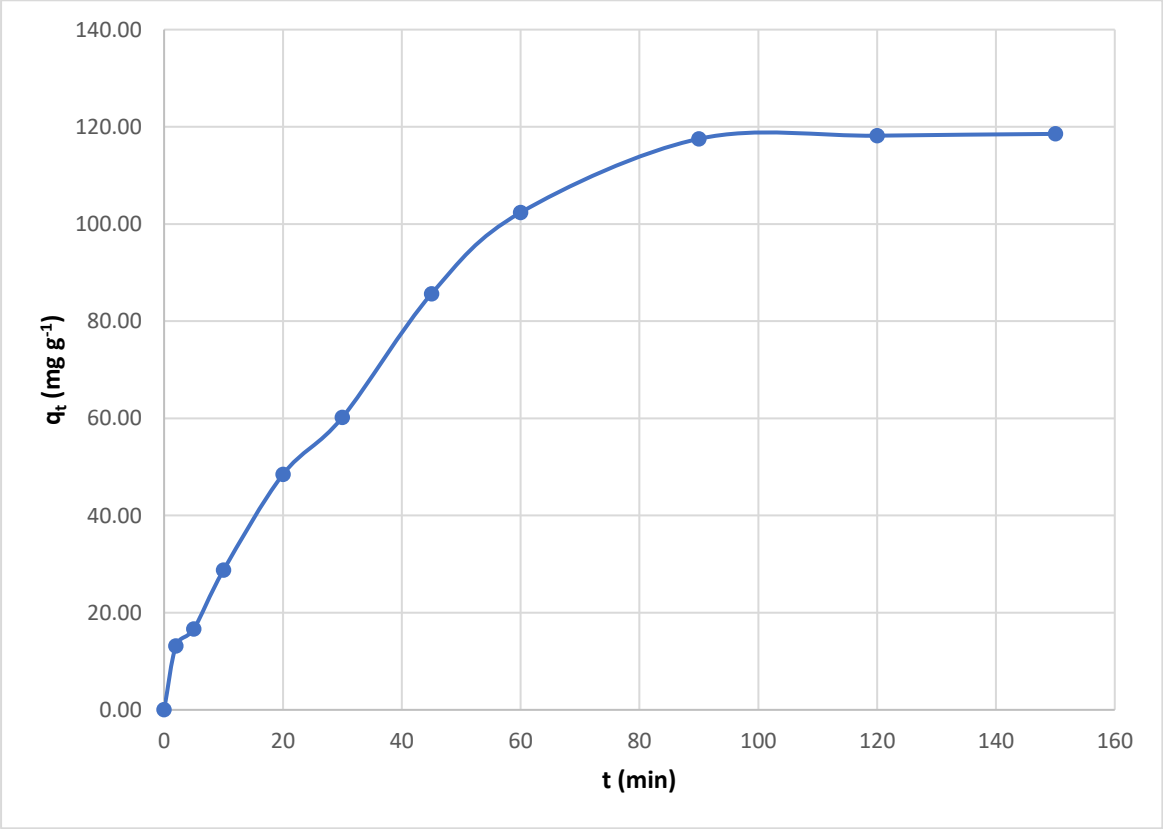

Fig. 4 The contact time trend of INC sorption onto the 10%V_2O_5@$MgAl_2O_4$ composite.

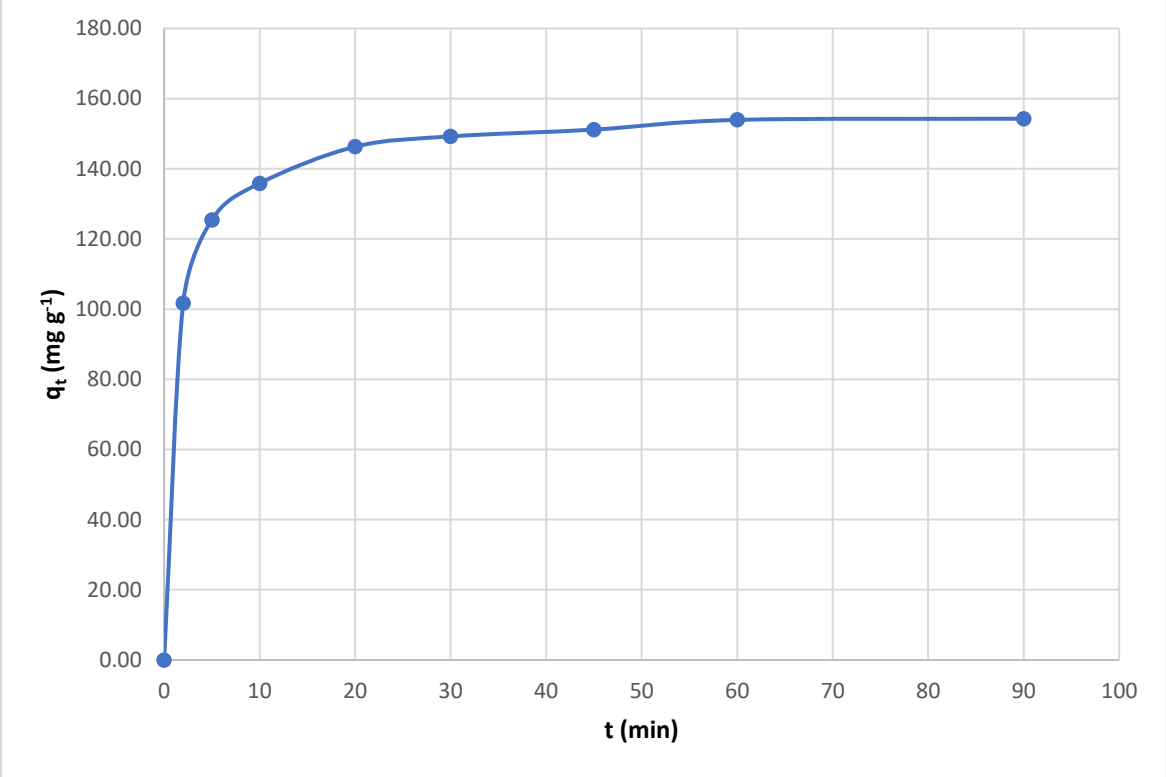

Fig. 5 The contact time trend of BFC sorption onto the $MgAl_2O_4$ nanocomposite.

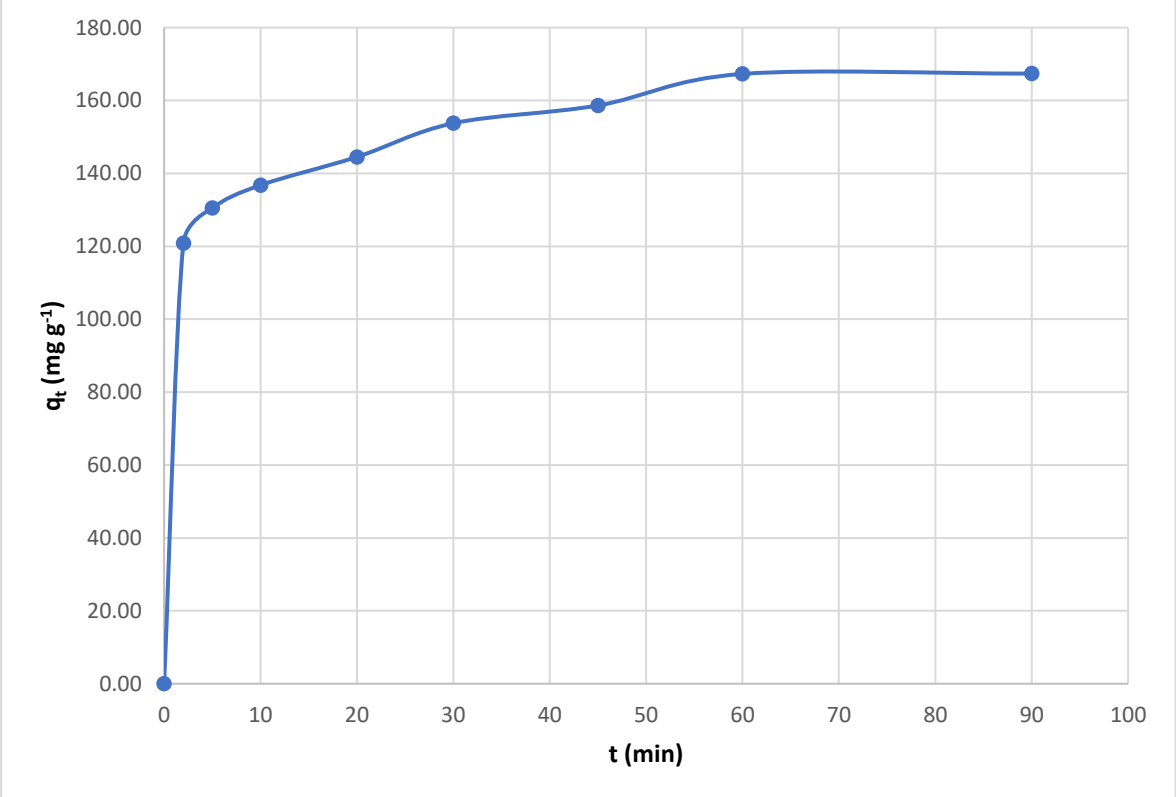

Fig. 6 The contact time trend of BFC sorption onto the 2.5%V_2O_5@$MgAl_2O_4$ composite.

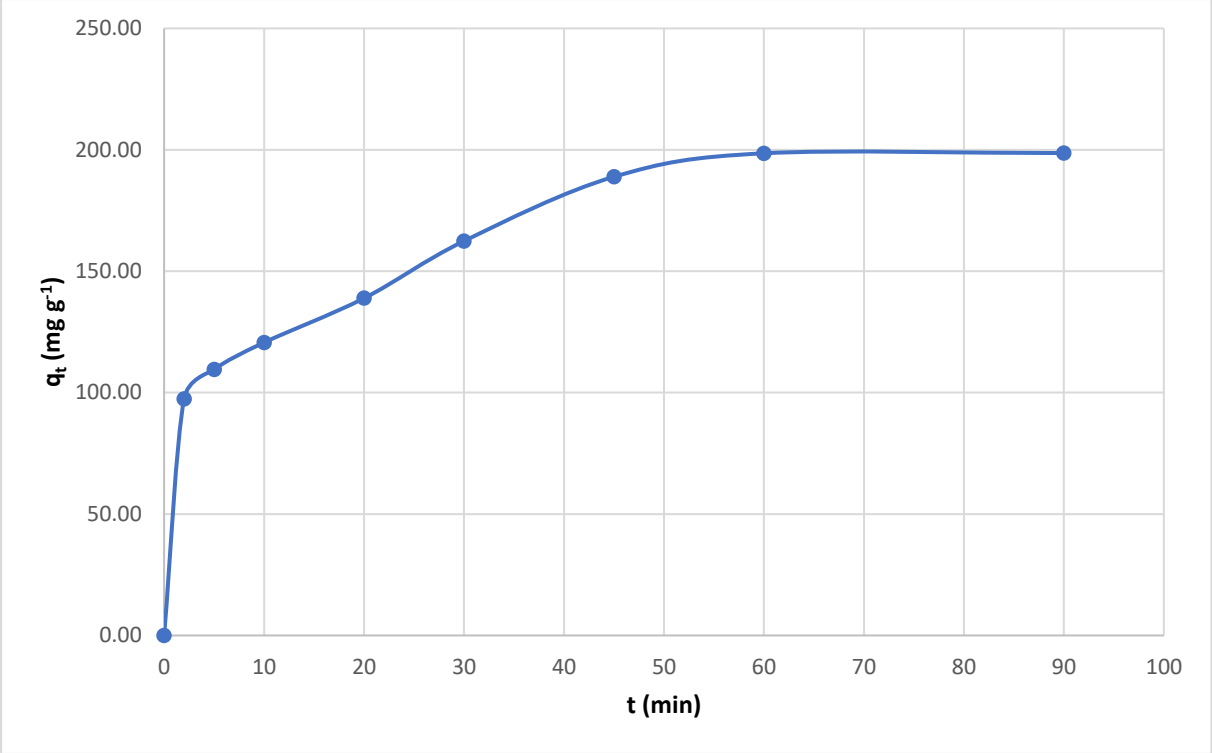

Fig. 7 The contact time trend of BFC sorption onto the 5%V_2O_5@$MgAl_2O_4$ composite.

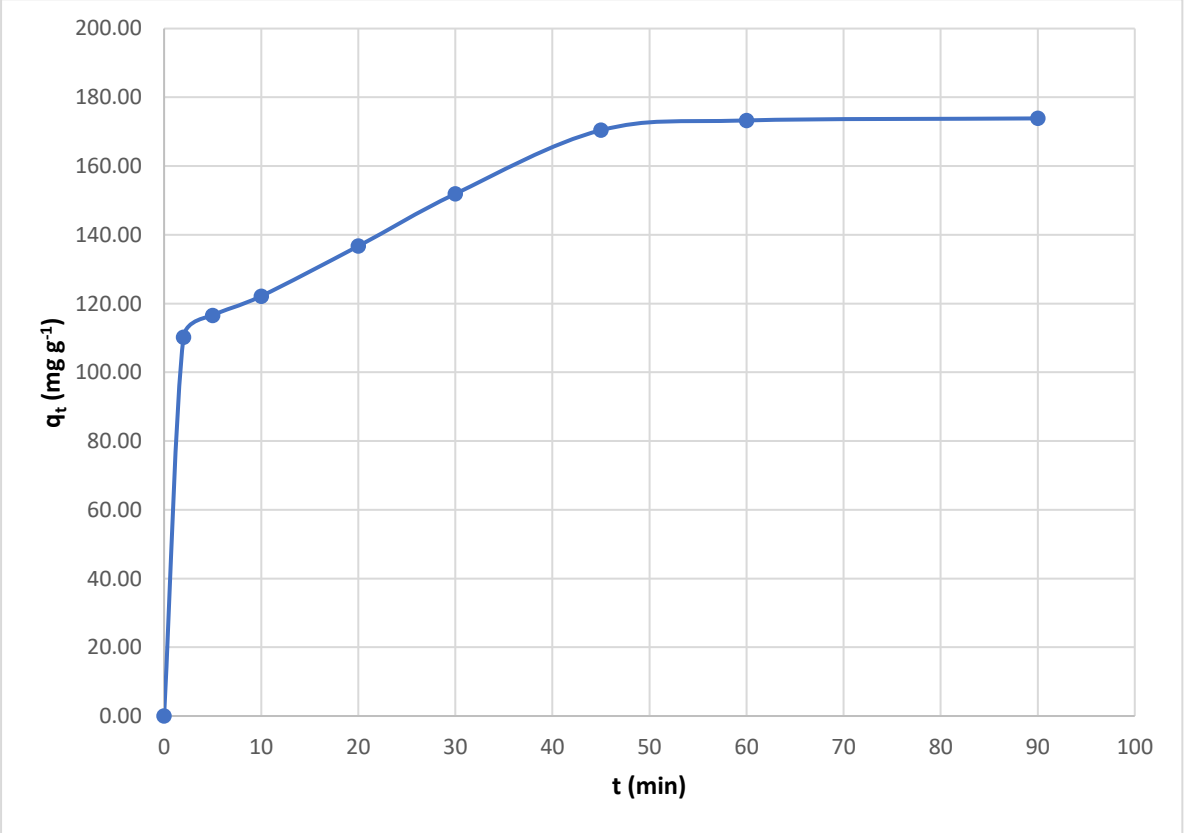

Fig. 8 The contact time trend of BFC sorption onto the 10%V_2O_5@$MgAl_2O_4$ composite.

3.2 Adsorption rate order

The adsorption rate order of INC and BFC removal by $MgAl_2O_4$, 2.5%V_2O_5@$MgAl_2O_4$, 5%V_2O_5@$MgAl_2O_4$, and 10%V_2O_5@$MgAl_2O_4$ was studied via pseudo-first-order (PF, Eq. 3) and pseudo-second-order (PS, Eq. 4) kinetic models.

$$\ln(q_e - q_t) = \ln q_e - k_1.t \quad (3)$$

$$\frac{1}{q_t} = \frac{1}{k_2.q_e^2 t} + \frac{1}{q_e} \quad (4)$$

The symbol q_e (mg g-1) represents the equilibrium adsorption capacity. The PF and PS constants are also time-dependent, with the former represented as k1 (min^{-1}) and the latter as k2 (g mg^{-1} min^{-1}). The PF plots of the INC adsorption onto $MgAl_2O_4$, 2.5%V_2O_5@$MgAl_2O_4$, 5%V_2O_5@$MgAl_2O_4$, and 10%V_2O_5@$MgAl_2O_4$ composites were depicted in Fig. 9, 10, 11, and 12, respectively. Fig. 13, 14, 15, and 16 showed the PF plots of OXTC removal by $MgAl_2O_4$, 2.5%V_2O_5@$MgAl_2O_4$, 5%V_2O_5@$MgAl_2O_4$, and 10%V_2O_5@$MgAl_2O_4$, respectively. Additionally, Fig.17, 18, 19, and 20 illustrated the PS plots of INC sorption onto $MgAl_2O_4$, 2.5%V_2O_5@$MgAl_2O_4$, 5%V_2O_5@$MgAl_2O_4$, and 10%V_2O_5@$MgAl_2O_4$, respectively, while Fig. 21, 22, 23, and 24 showed the PS plots of BFC, respectively. The rate-order output of INC removals gathered in Table 1 illustrated that the sorption on four sorbents fitted the PS. Additionally, the BFC rate investigation output (Table 2) revealed the agreement of BFC sorption onto the $MgAl_2O_4$ and 2.5%V_2O_5@$MgAl_2O_4$ to

the PF, while its sorpion onto 5%V_2O_5@$MgAl_2O_4$ and 10%V_2O_5@$MgAl_2O_4$ fitted the PF.

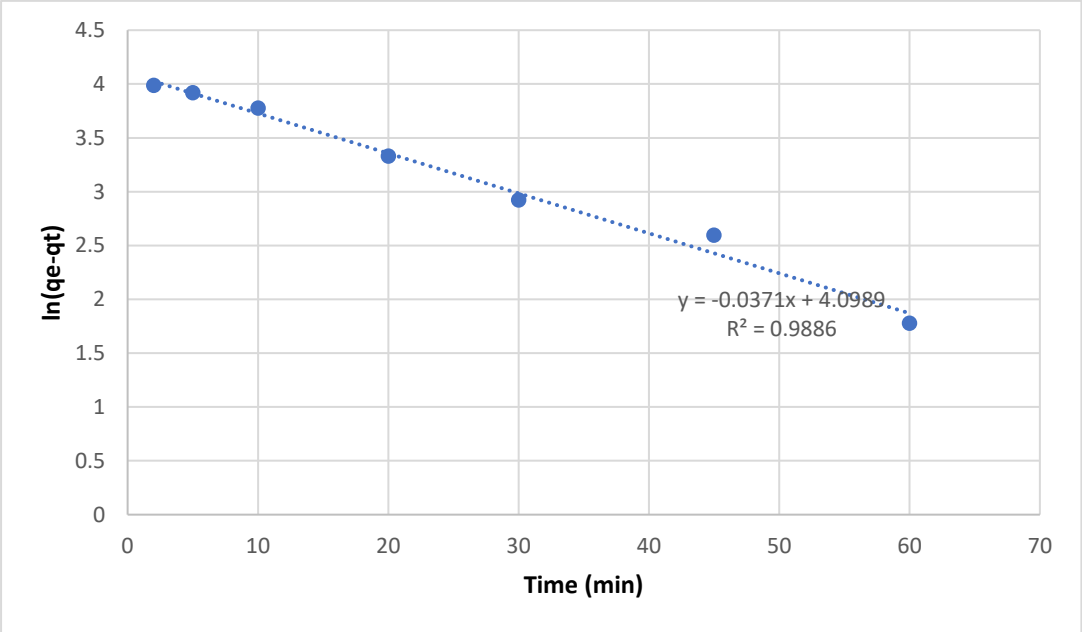

Fig. 9 The PF investigation of INC sorption onto $MgAl_2O_4$ composite.

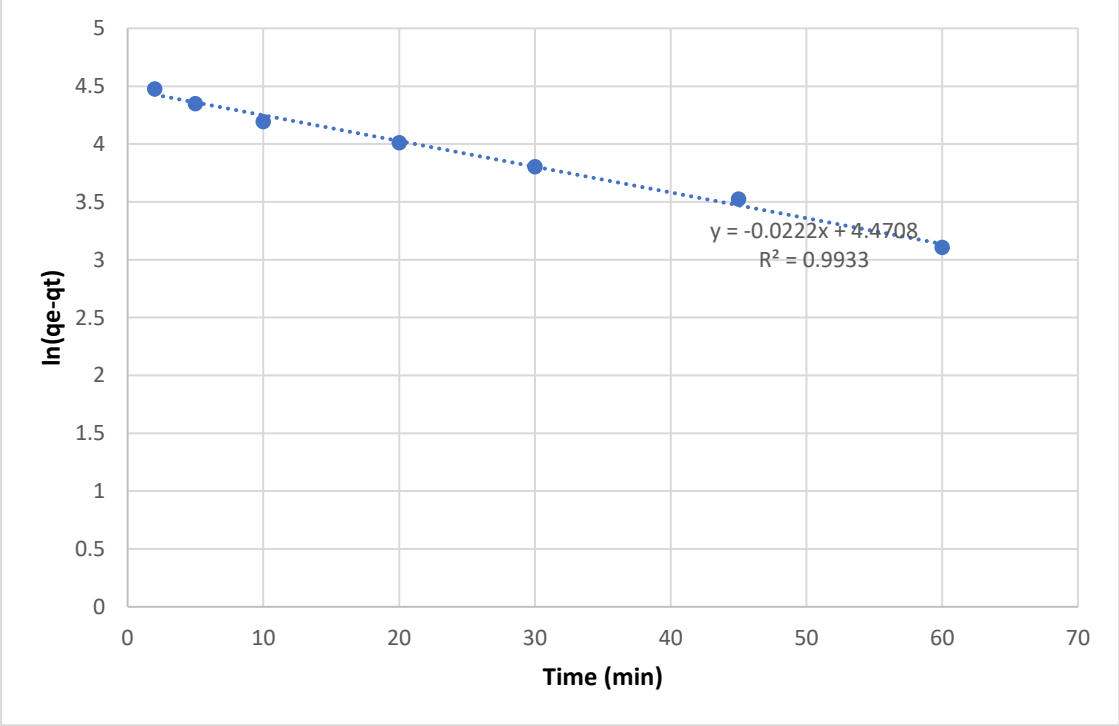

Fig. 10 The PF investigation of INC sorption onto 2.5%V_2O_5@$MgAl_2O_4$ composite.

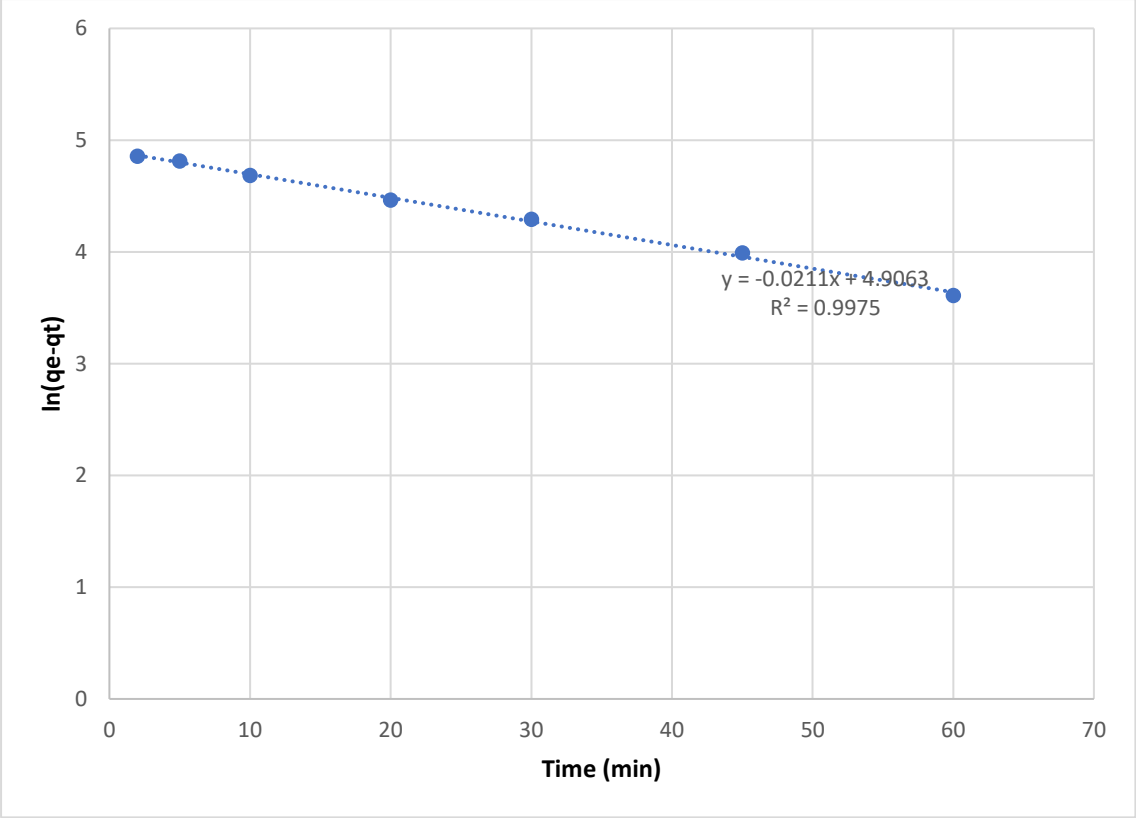

Fig. 11 The PF investigation of INC sorption onto $5\%V_2O_5@MgAl_2O_4$ composite.

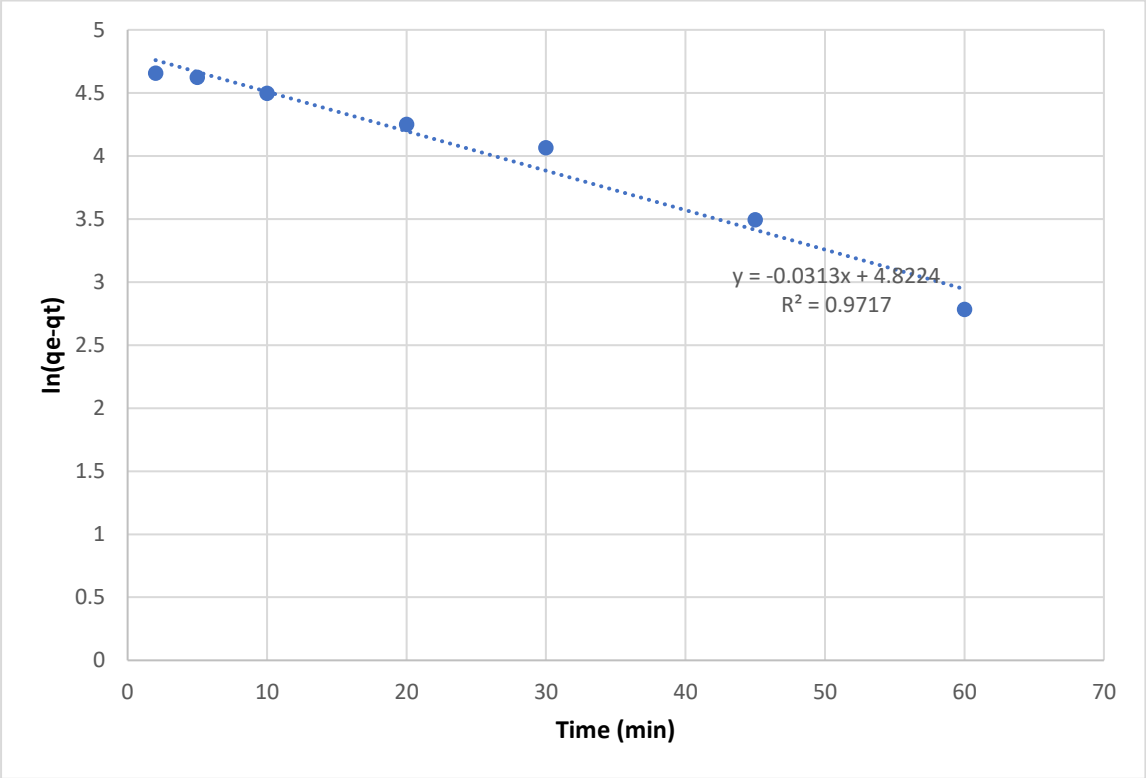

Fig. 12 The PF investigation of INC sorption onto $10\%V2O5@MgAl_2O_4$ composite.

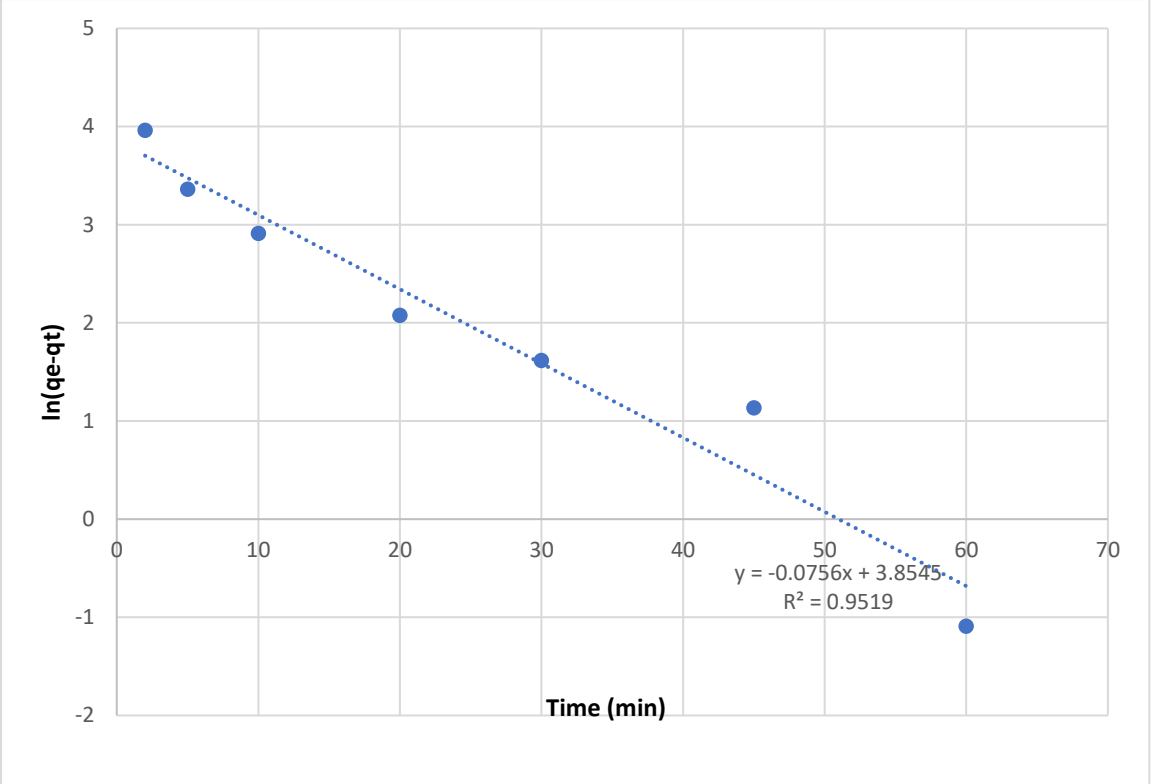

Fig. 13 The PF investigation of BFC sorption onto $MgAl_2O_4$ composite.

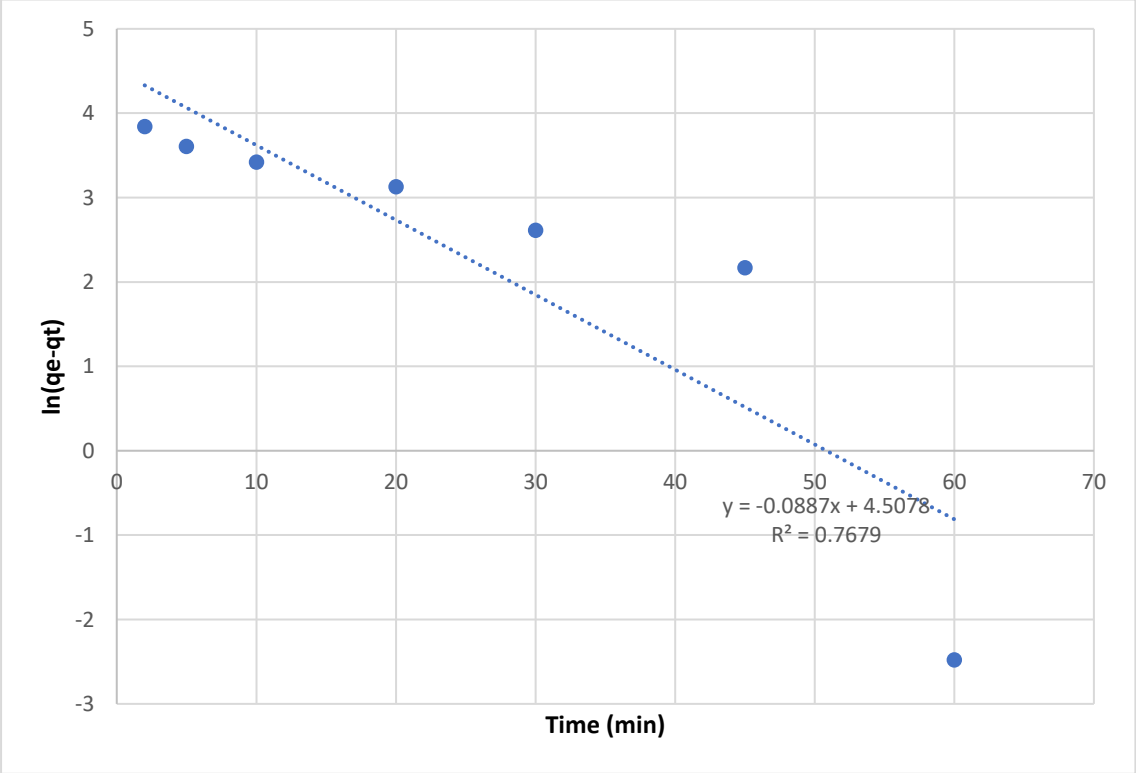

Fig. 14 The PF investigation of BFC sorption onto $2.5\%V2O5@MgAl_2O_4$ composite.

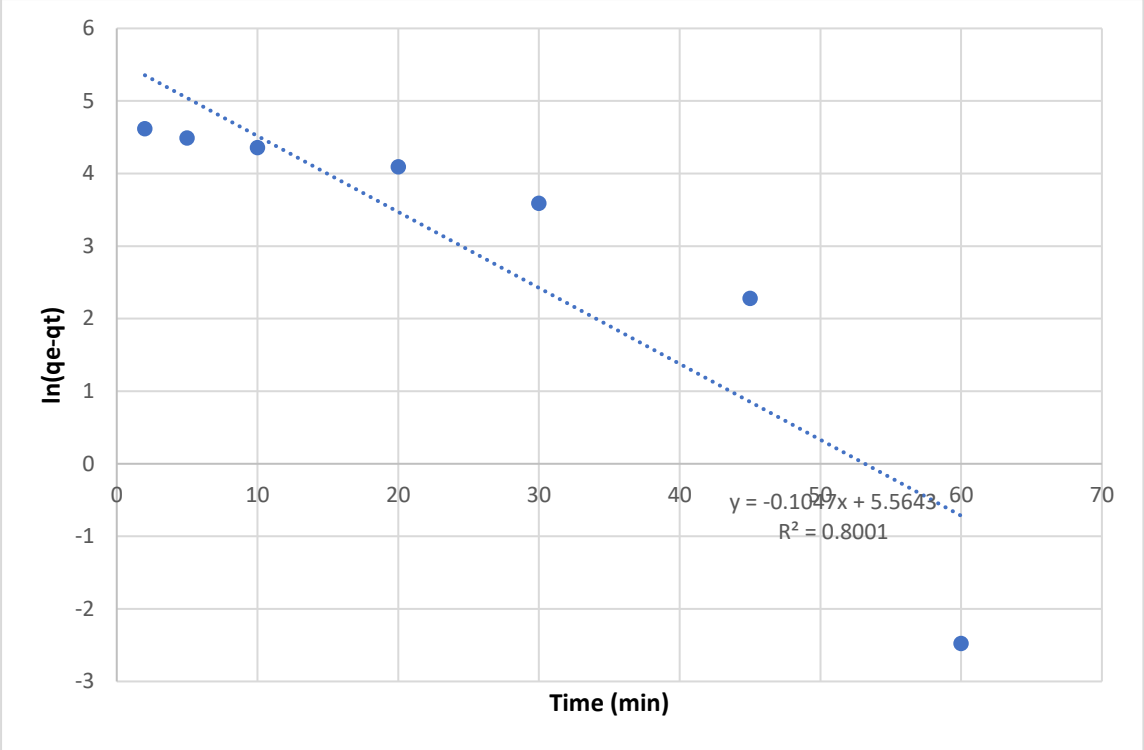

Fig. 15 The PF investigation of BFC sorption onto 5%V2O5@$MgAl_2O_4$ composite.

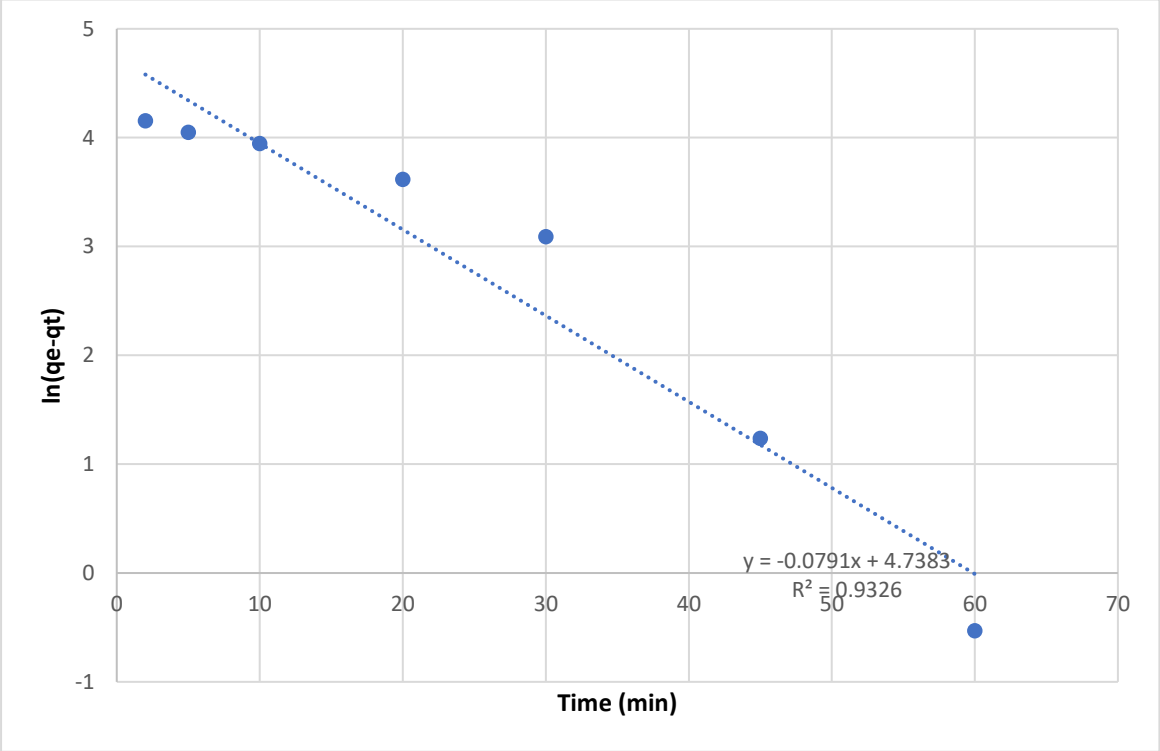

Fig. 16 The PF investigation of BFC sorption onto 10%V2O5@$MgAl_2O_4$ composite.

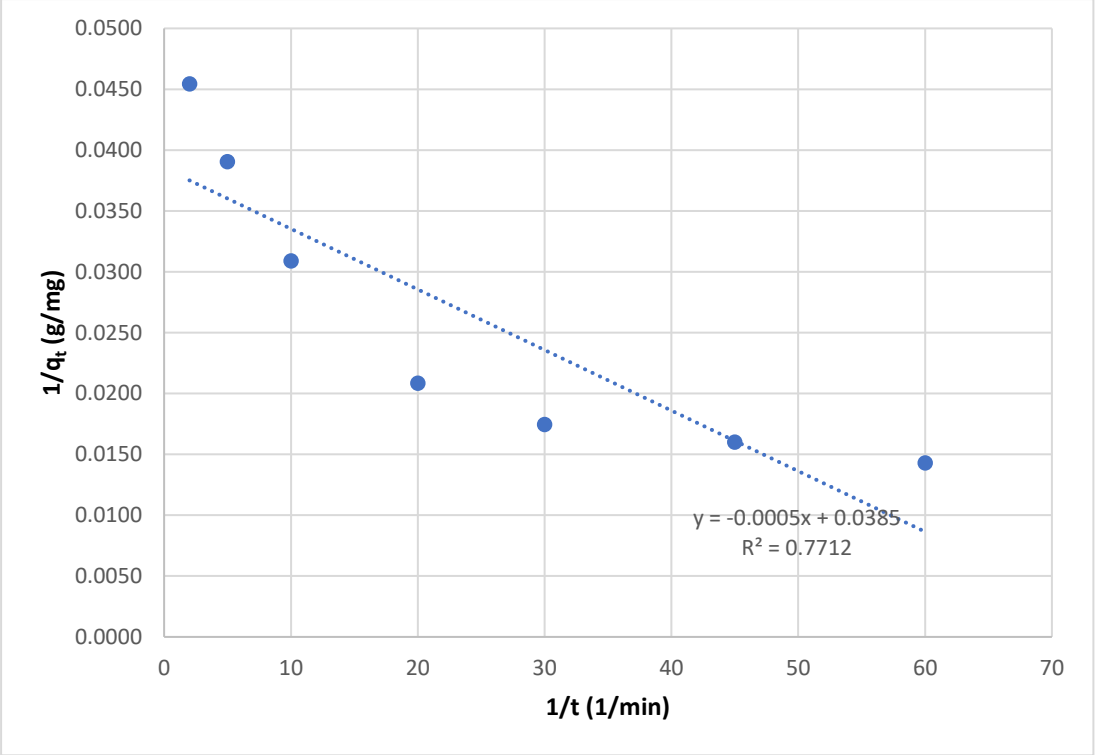

Fig. 17 The PS investigation of INC sorption onto $MgAl_2O_4$ composite.

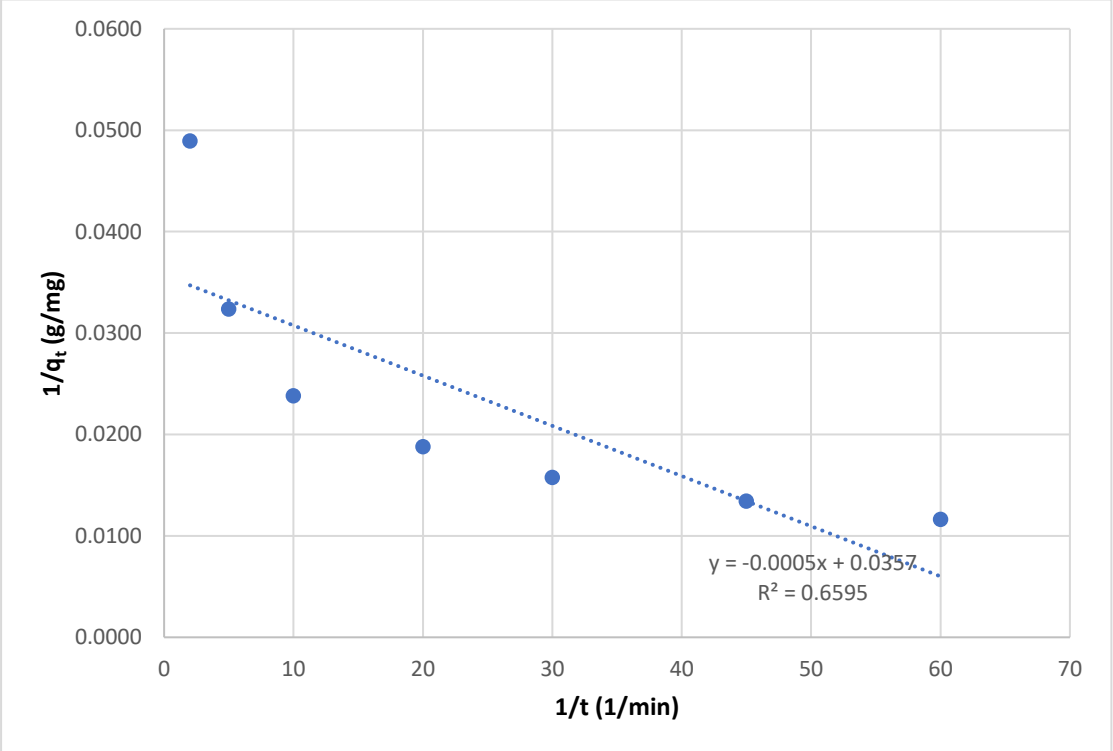

Fig. 18 The PS investigation of INC sorption onto $2.5\%V2O5@MgAl_2O_4$ composite.

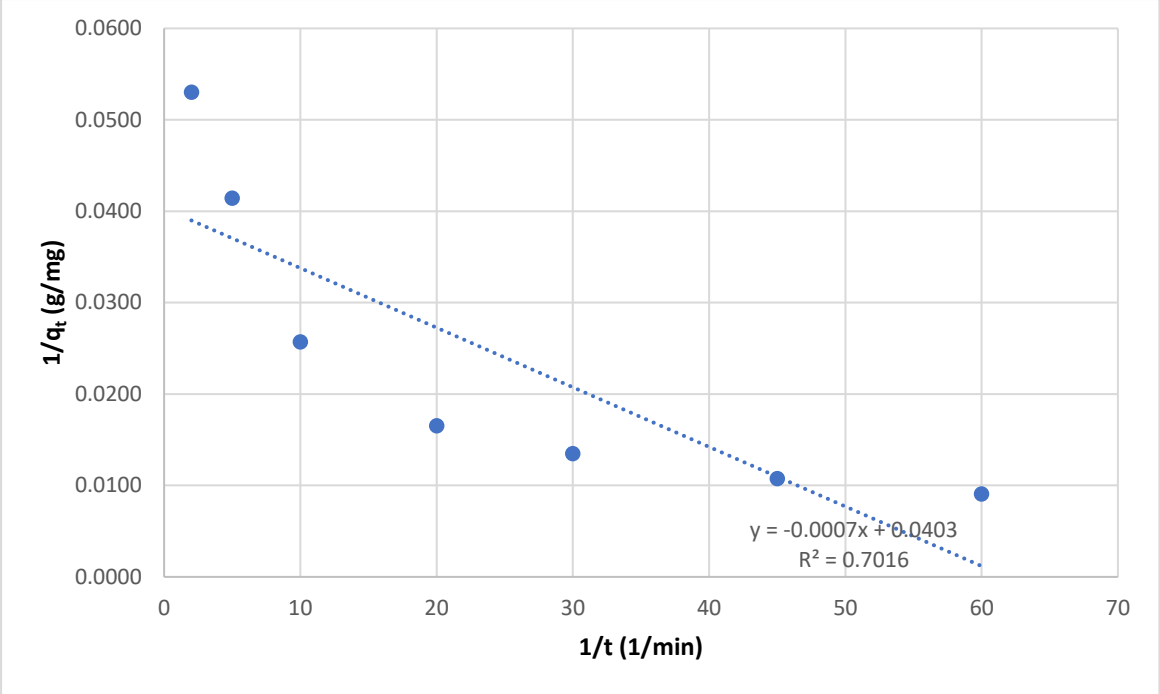

Fig. 19 The PS investigation of INC sorption onto 5%V_2O_5@$MgAl_2O_4$ composite.

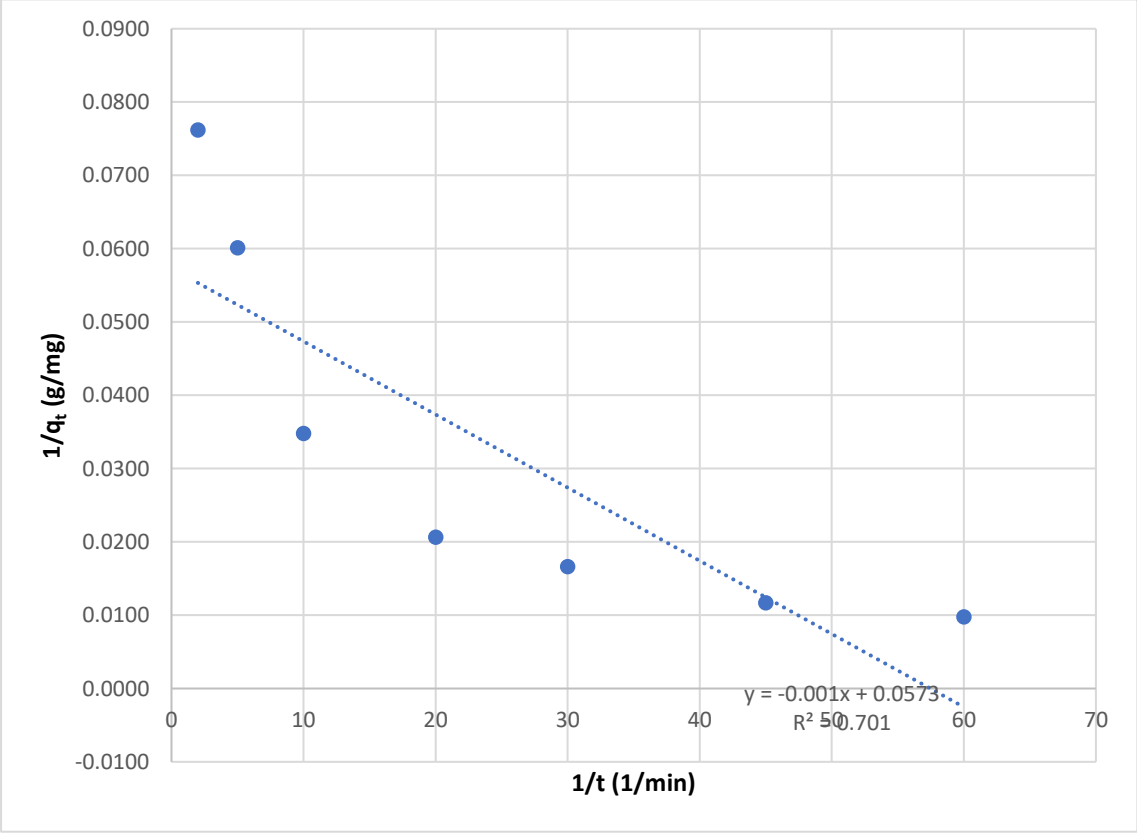

Fig. 20 The PS investigation of INC sorption onto 10%V2O5@$MgAl_2O_4$ composite.

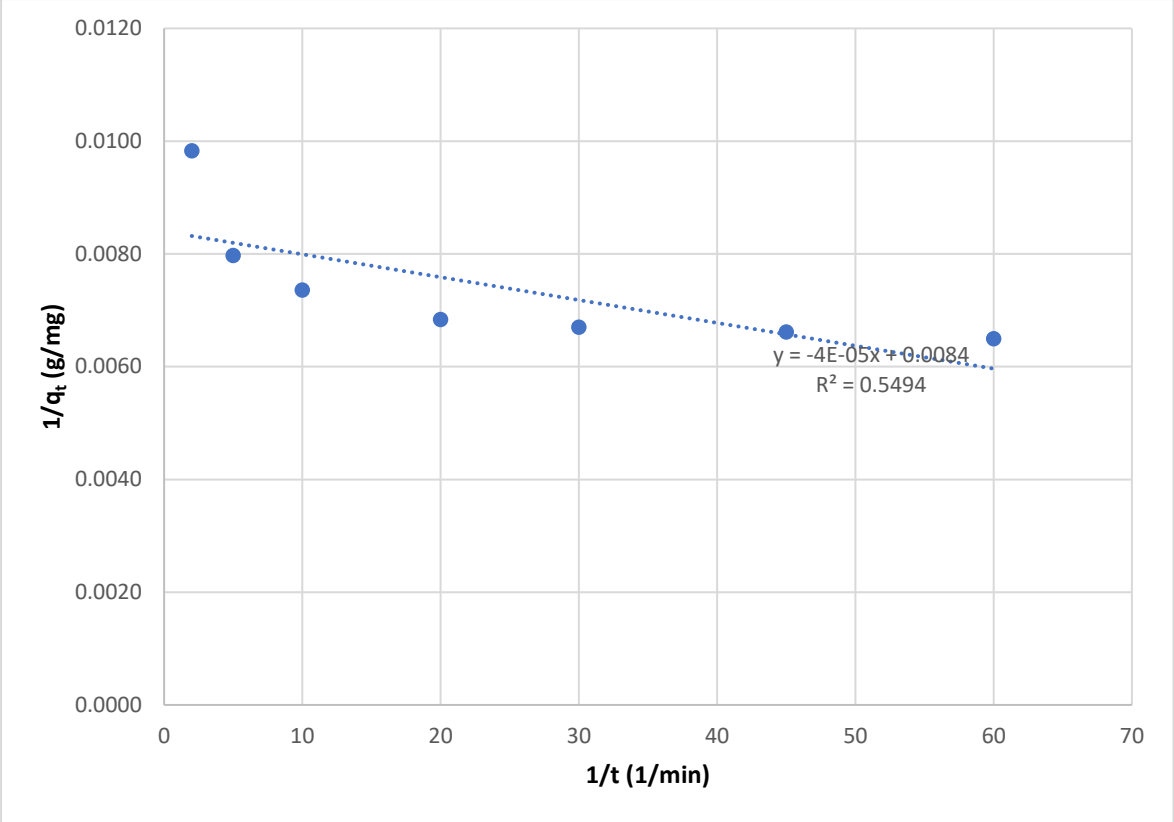

Fig. 21 The PS investigation of BFC sorption onto $MgAl_2O_4$ composite.

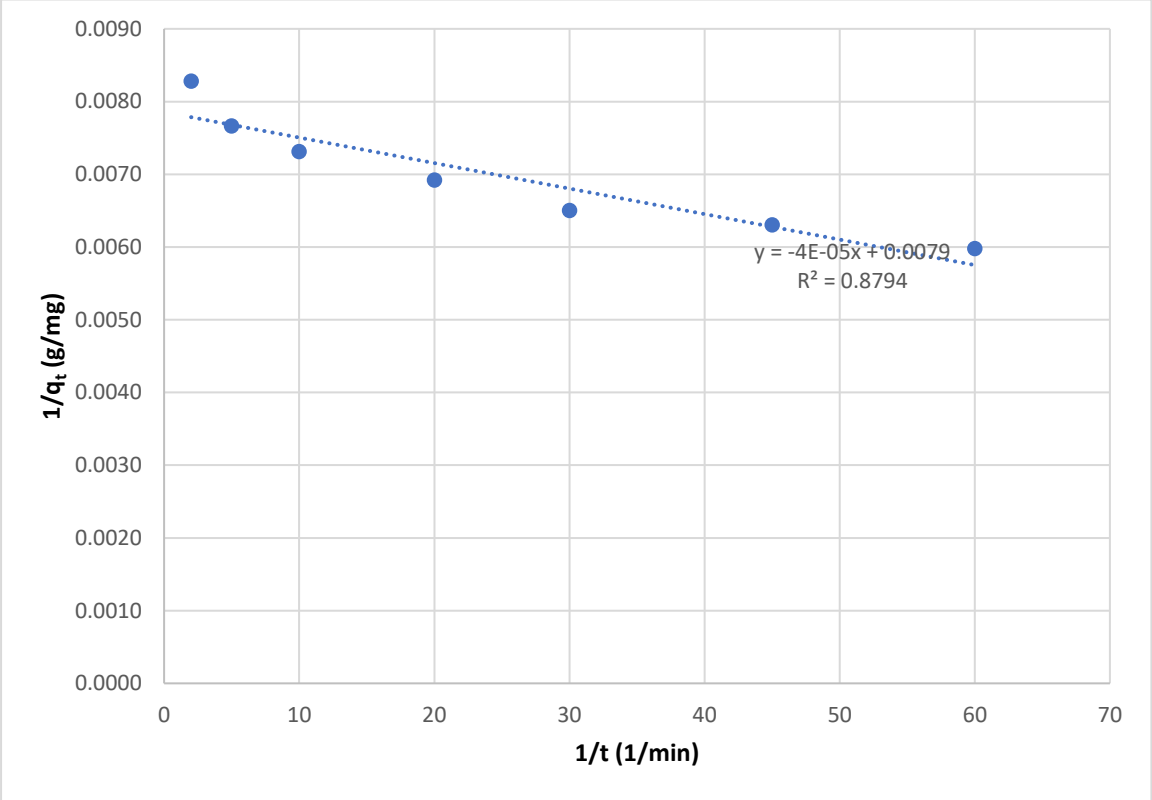

Fig. 22 The PS investigation of BFC sorption onto $2.5\%V2O5@MgAl_2O_4$ composite.

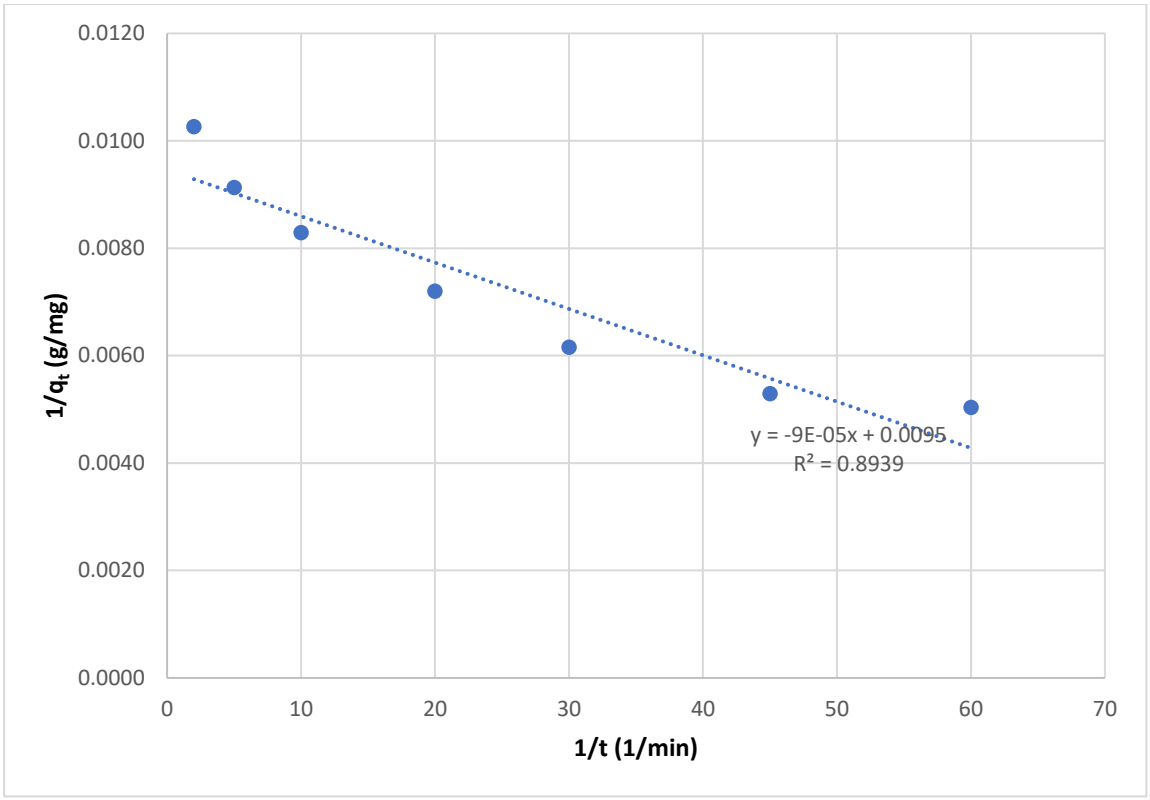

Fig. 23 The PS investigation of BFC sorption onto 5%V2O5@$MgAl_2O_4$ composite.

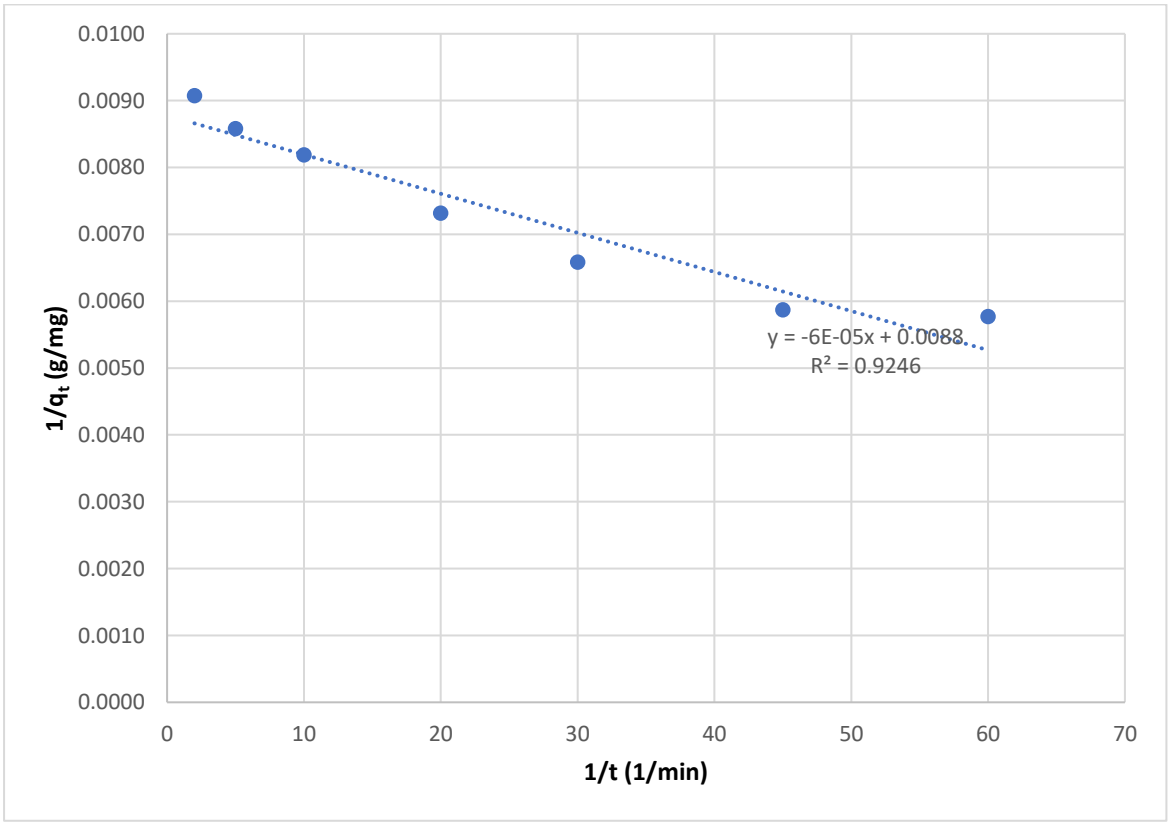

Fig. 24 The PS investigation of BFC sorption onto 10%V2O5@$MgAl_2O_4$ composite.

Table 1 The adsorption rate order results of INC removal by $MgAl_2O_4$, 2.5%V2O5@$MgAl_2O_4$, 5%V2O5@$MgAl_2O_4$, and 10%V2O5@$MgAl_2O_4$.

Adsorbent	qe exp. (mg g^{-1})	*PFO*		*PSO*	
		R^2	k_1	R^2	k_2
AlMgO4	75.91	0.9852	0.0536	0.9448	0.006
2.5%V2O5@AlMgO4	108.37	0.9882	0.0343	0.9598	0.003
5%V2O5@AlMgO4	147.30	0.9978	0.0214	0.8231	0.002
10%V2O5@AlMgO4	118.54	0.9810	0.0202	0.7671	0.002

Table 2 The adsorption rate order results of BFC removal by $MgAl_2O_4$, 2.5%V2O5@$MgAl_2O_4$, 5%V2O5@$MgAl_2O_4$, and 10%V2O5@$MgAl_2O_4$.

Adsorbent	qe exp. (mg g-1)	PFO		PSO	
		R2	k1	R2	k2
AlMgO4	154.27	0.9519	0.0536	0.9923	0.006
2.5%V2O5@AlMgO4	167.38	0.7679	0.0756	0.7890	0.010
5%V2O5@AlMgO4	198.65	0.8001	0.0887	0.7399	0.004
10%V2O5@AlMgO4	173.85	0.9326	0.1047	0.6489	0.007

3.3 Adsorption control mechanism

It is believed that there are two steps to the adsorption process, the first of which is the movement of adsorbate molecules from a liquid to a solid sorbent surface. Step two involves getting the sorbate molecules to go deep into the sorbent. The rate control mechanism, the slowest sorption step, determines the adsorption rate. The rate-control mechanism of INC and BFC removal by $MgAl_2O_4$, 2.5%V_2O_5@$MgAl_2O_4$, 5%V_2O_5@$MgAl_2O_4$, and 10%V_2O_5@$MgAl_2O_4$ was studied via using the intraparticle (IPD, Eq. 5) and the liquid-film (LFD, Eq. 6) diffusion model.

$$q_t = K_{IP} * t^{\frac{1}{2}} + C_i \quad (5)$$

$$\ln(1 - F) = -K_{LF} * t \quad (6)$$

The IPD constant is denoted by K_{IPD} (mg g^{-1} $min^{-1/2}$), and the LFD constant is designated by K_{LFD} (min^{-1}). C_i: the boundary layer factor, expressed as mg g^{-1}. The LFD plots of the INC adsorption onto $MgAl_2O_4$, 2.5%V_2O_5@$MgAl_2O_4$, 5%V_2O_5@$MgAl_2O_4$, and 10%V_2O_5@$MgAl_2O_4$ composites were depicted in Fig. 25, 26, 27, and 28, respectively. Fig. 29, 30, 31, and 32 showed the LFD plots of OXTC removal by $MgAl_2O_4$, 2.5%V_2O_5@$MgAl_2O_4$, 5%V_2O_5@$MgAl_2O_4$, and 10%V_2O_5@$MgAl_2O_4$, respectively. Additionally, Fig. 33, 34, 35, and 36 illustrated the IPD plots of INC sorption onto $MgAl_2O_4$, 2.5%V_2O_5@$MgAl_2O_4$, 5%V_2O_5@$MgAl_2O_4$, and 10%V_2O_5@$MgAl_2O_4$, respectively, while Fig. 37, 38, 39, and 40 showed the IPD plots of BFC,

respectively. The rate-control output of INC removal (Table 3) illustrated that the LFD controlled the sorption on 5%V_2O_5@$MgAl_2O_4$ and 10%V_2O_5@$MgAl_2O_4$, while IPD controlled it on $MgAl_2O_4$, and 2.5%V_2O_5@$MgAl_2O_4$. As for the BFC outputs (Table 4), it revealed that IPD controlled the of BFC sorption onto all sorbent except of the $MgAl_2O_4$.

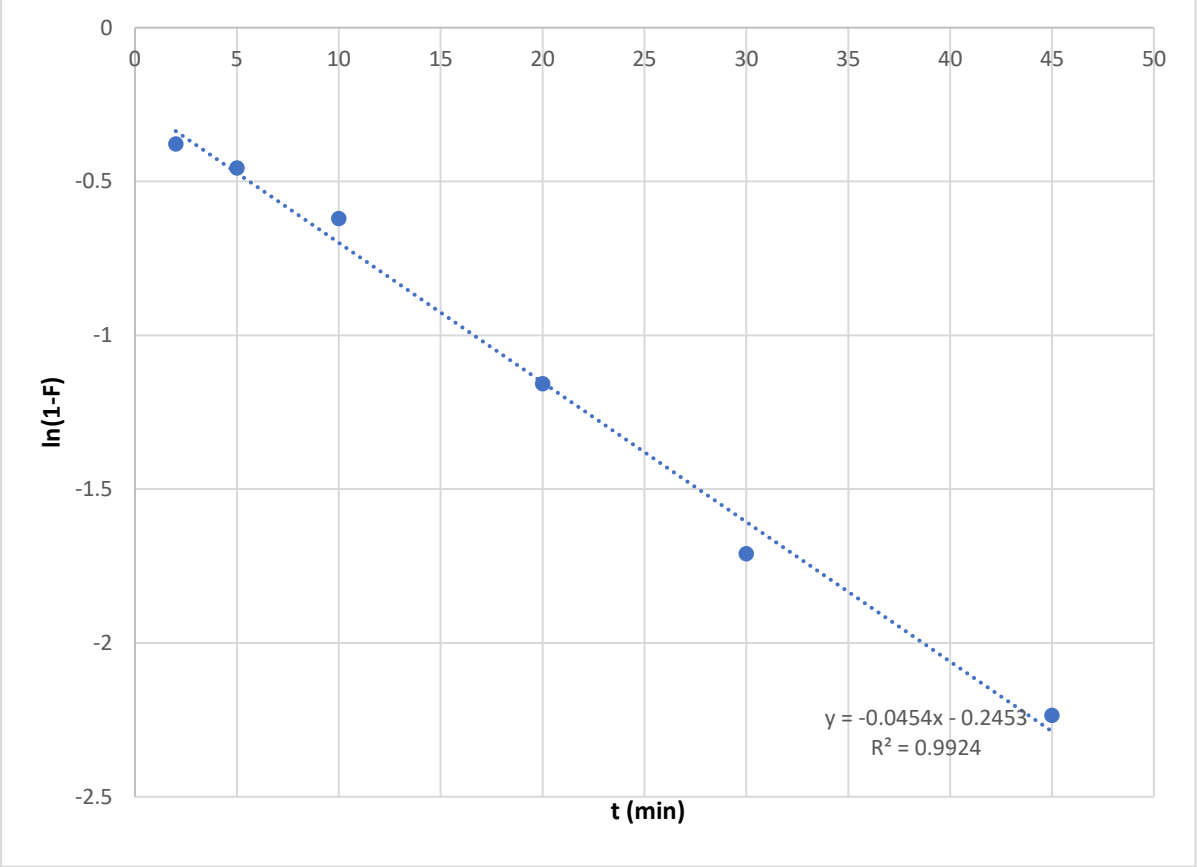

Fig. 25 The LFD investigation of INC sorption onto $MgAl_2O_4$ composite.

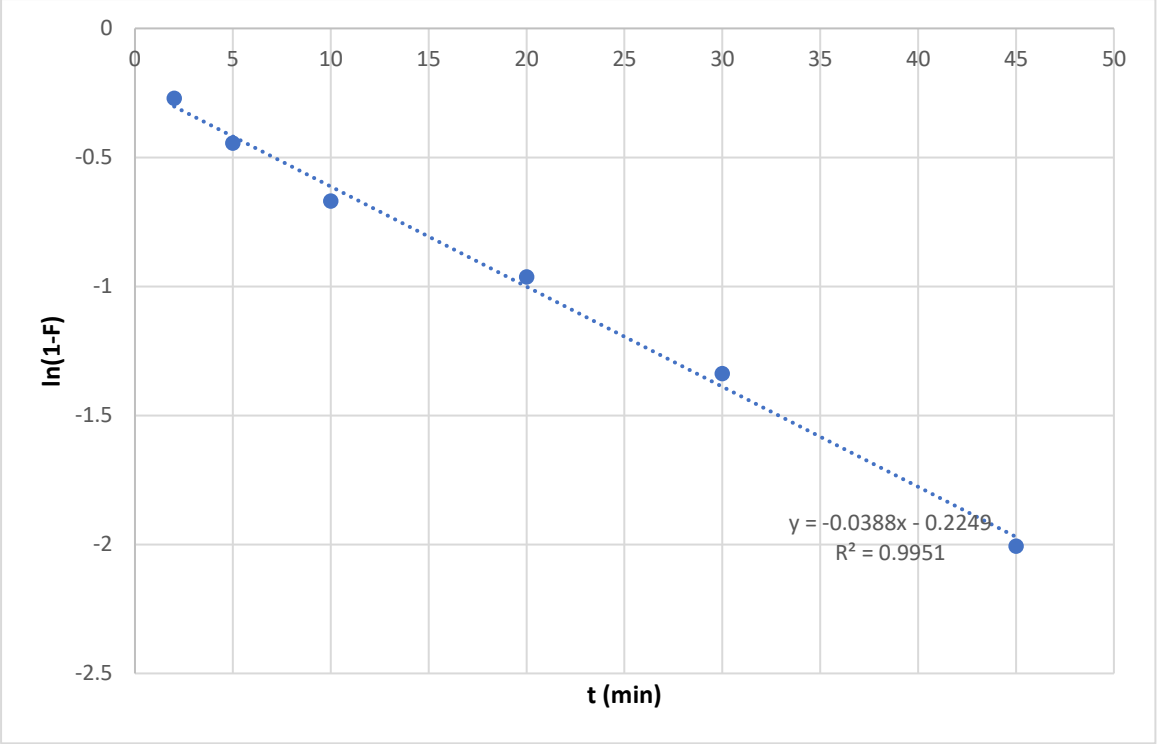

Fig. 26 The LFD investigation of INC sorption onto 2.5%V2O5@$MgAl_2O_4$ composite.

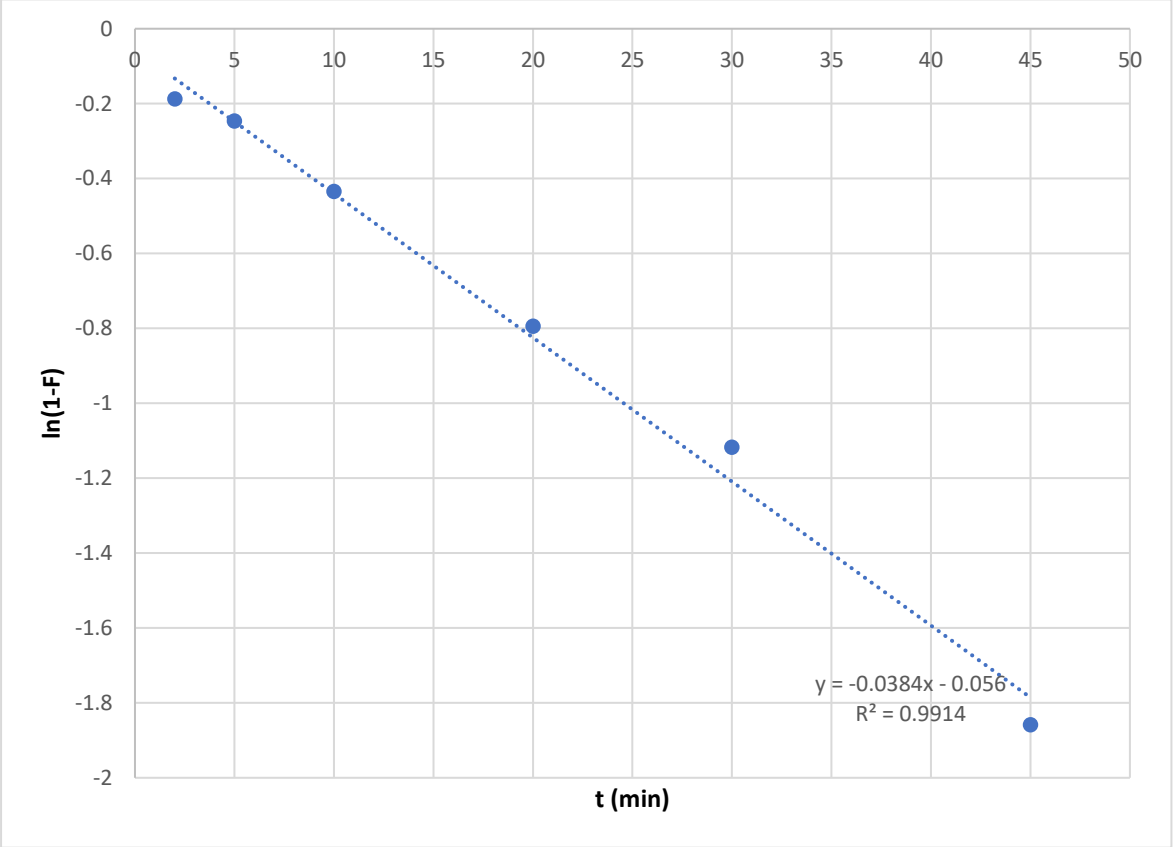

Fig. 27 The LFD investigation of INC sorption onto 5%V2O5@$MgAl_2O_4$ composite.

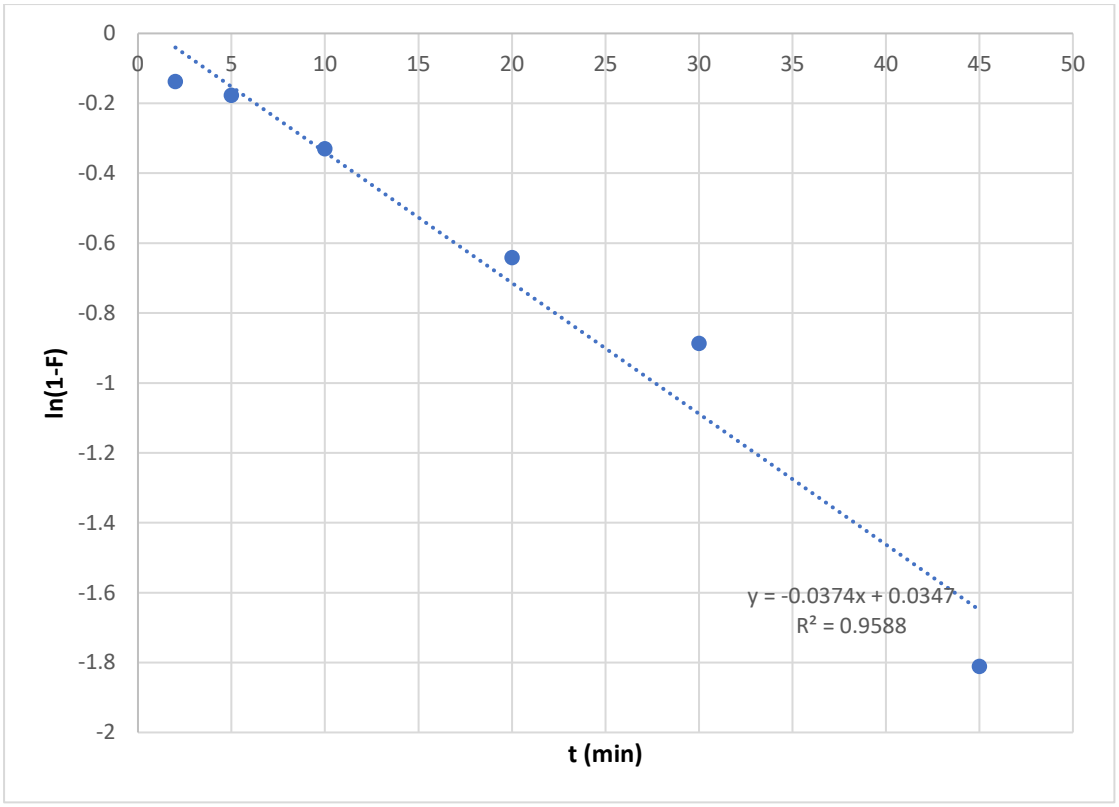

Fig. 28 The LFD investigation of INC sorption onto 10%V2O5@$MgAl_2O_4$ composite.

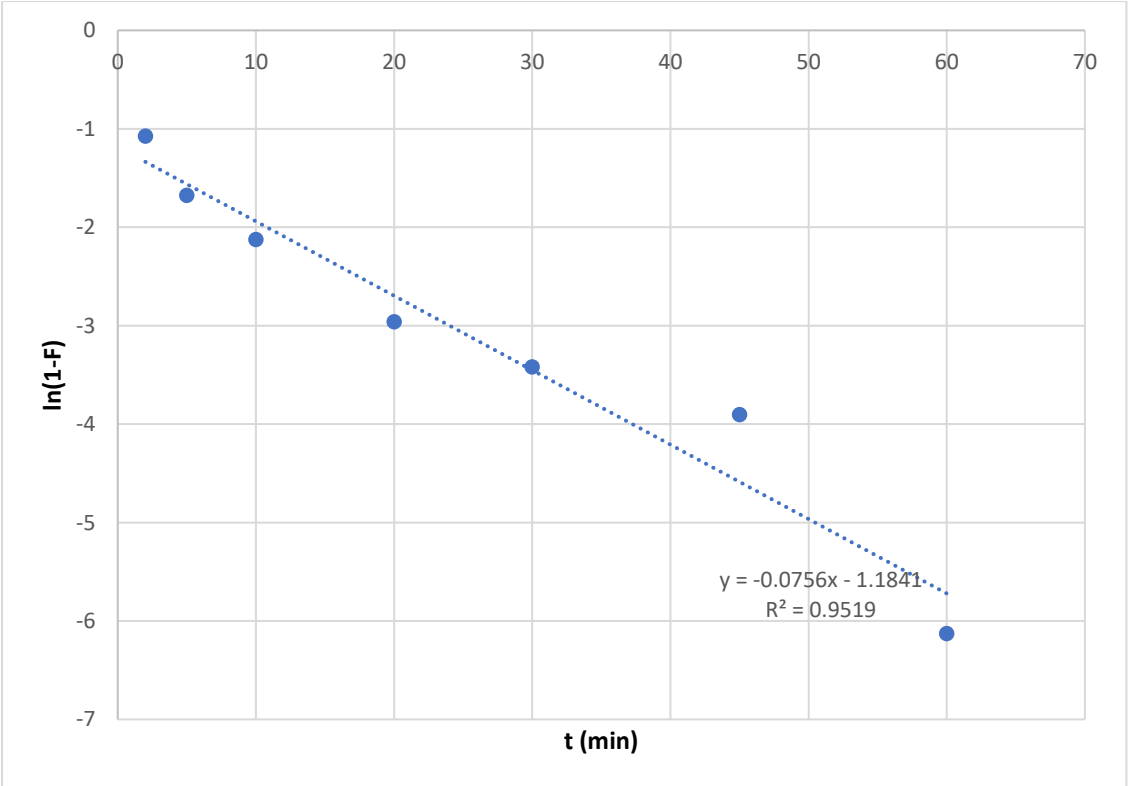

Fig. 29 The LFD investigation of BFC sorption onto $MgAl_2O_4$ composite.

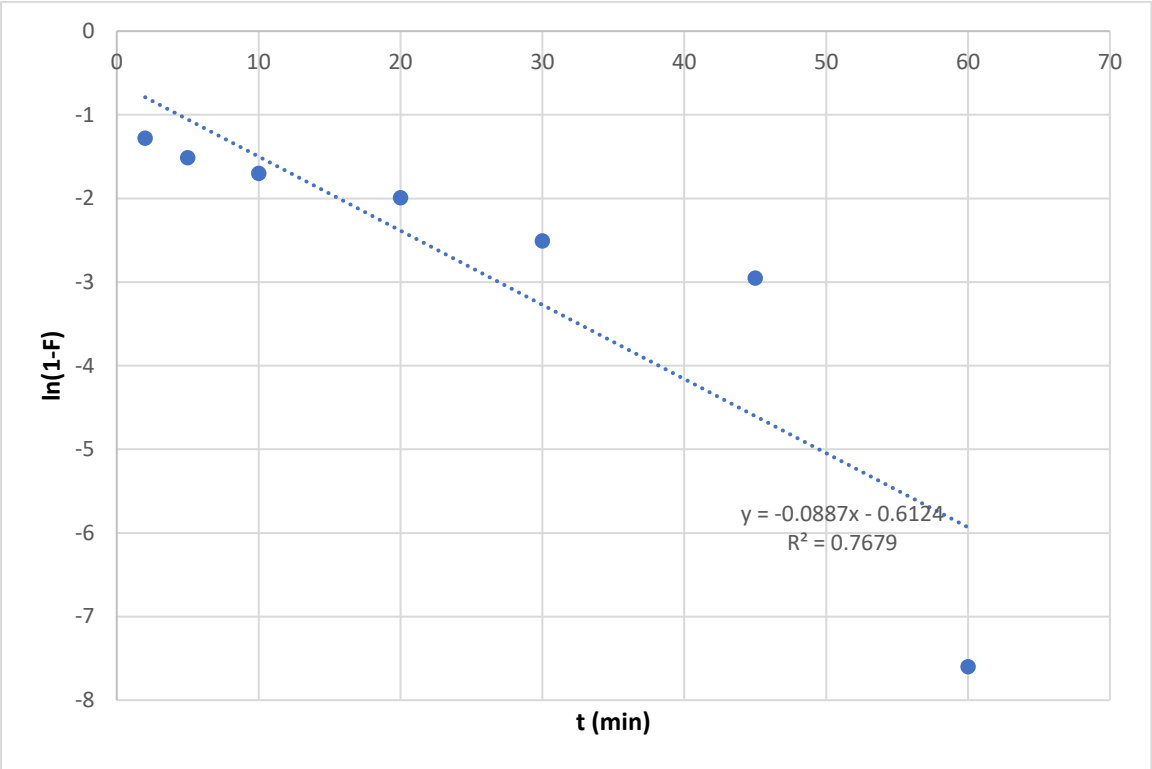

Fig. 30 The LFD investigation of BFC sorption onto 2.5%V2O5@$MgAl_2O_4$ composite.

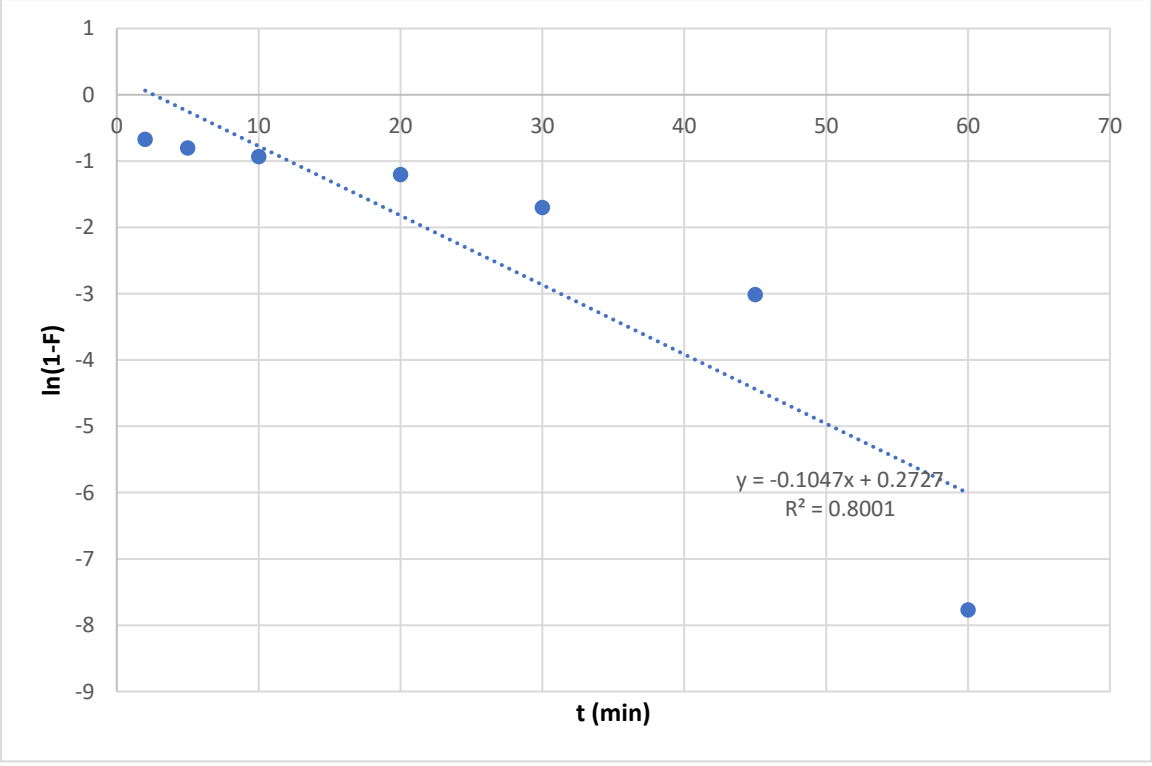

Fig. 31 The LFD investigation of BFC sorption onto 5%V2O5@$MgAl_2O_4$ composite.

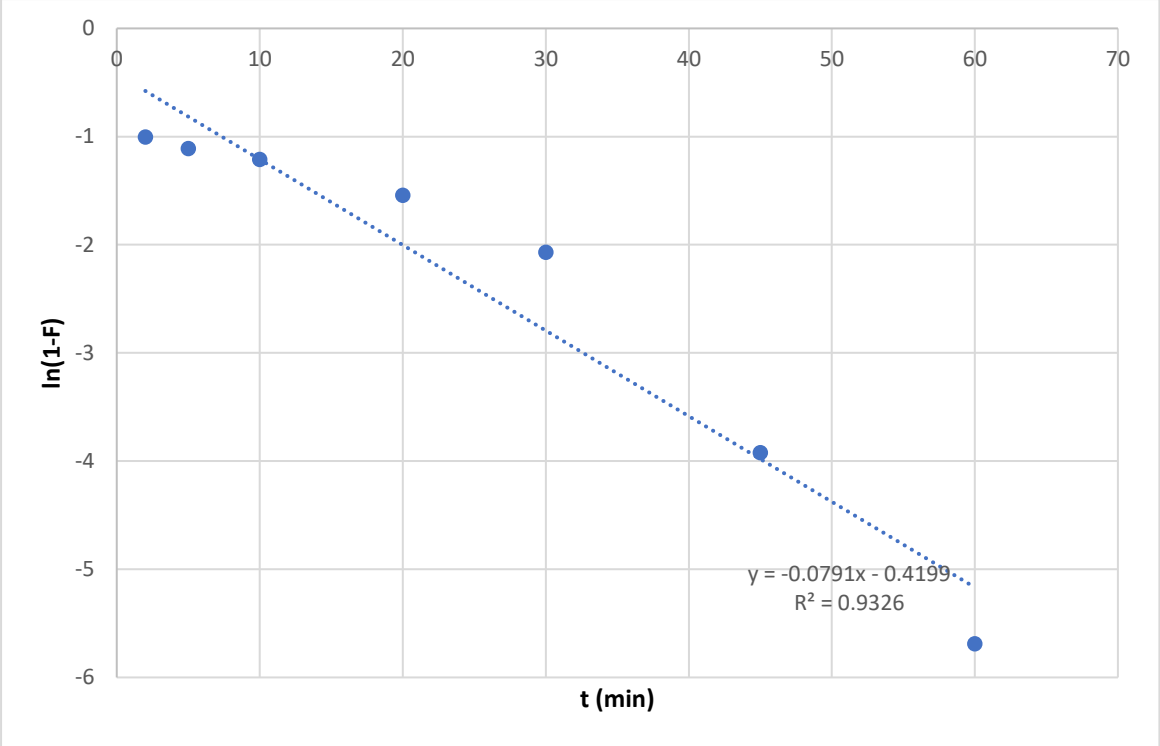

Fig. 32 The LFD investigation of BFC sorption onto 10%V2O5@$MgAl_2O_4$ composite.

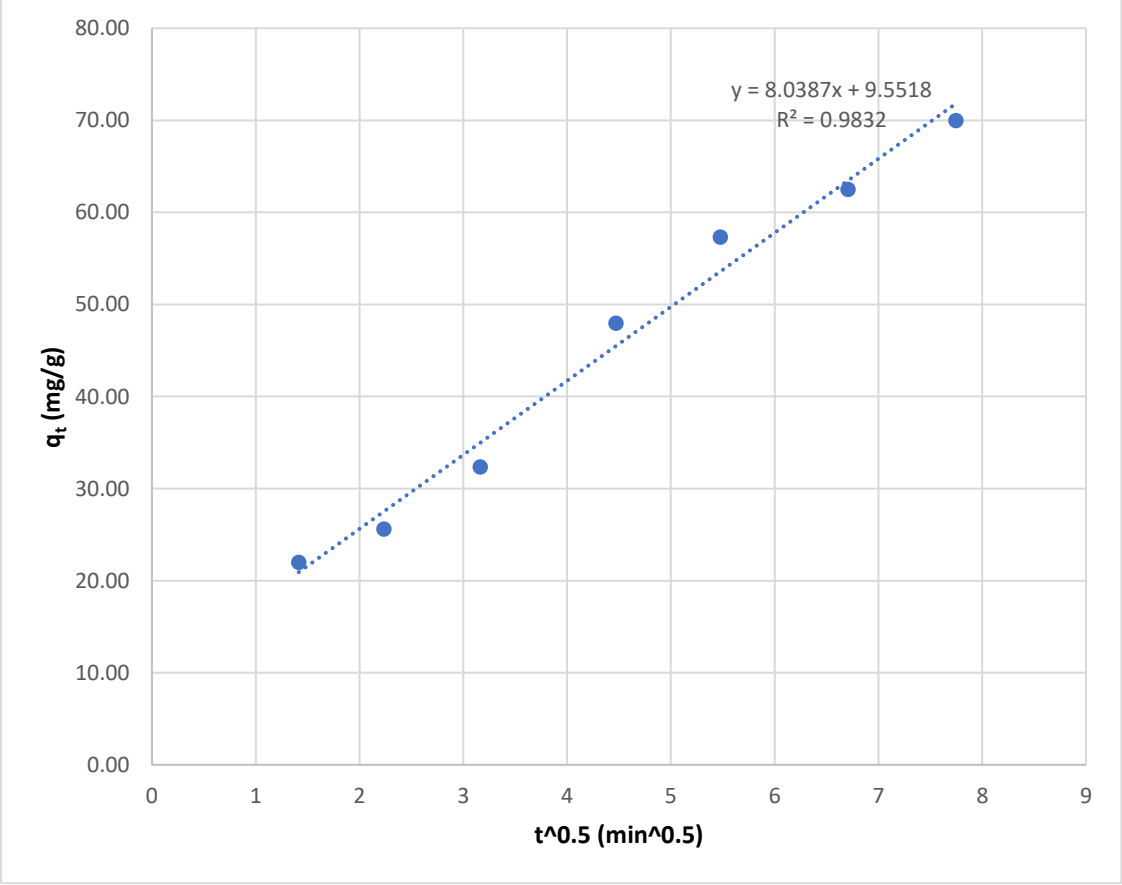

Fig. 33 The IPD investigation of INC sorption onto $MgAl_2O_4$ composite.

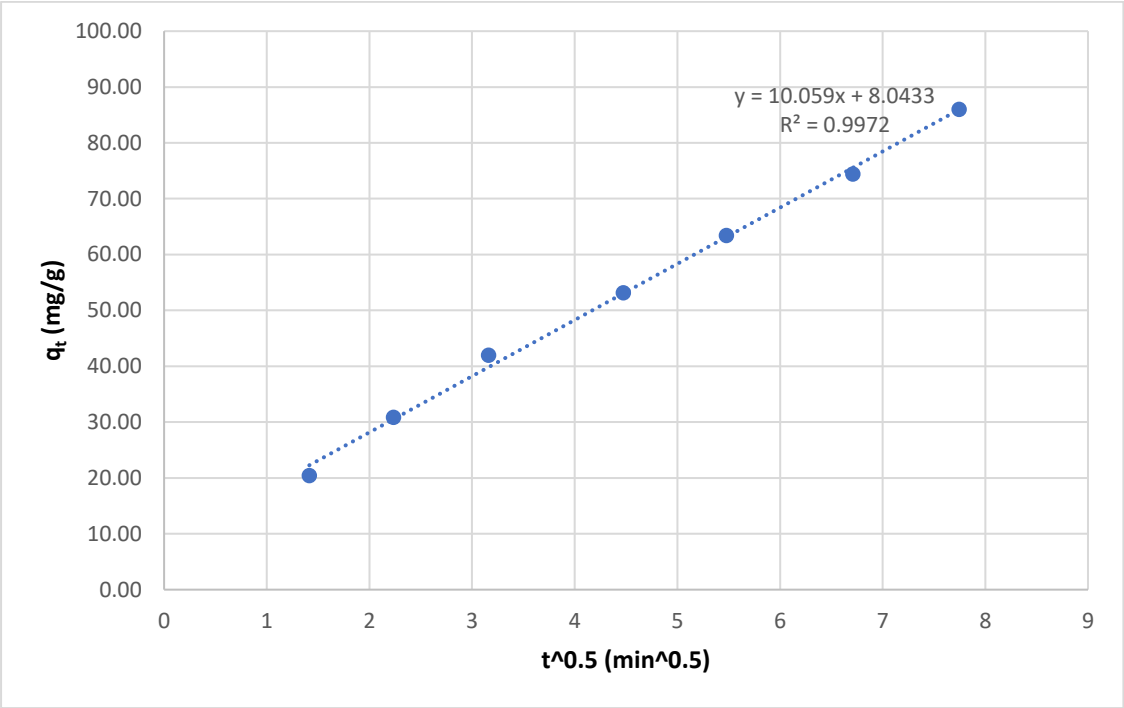

Fig. 34 The IPD investigation of INC sorption onto 2.5%V2O5@$MgAl_2O_4$ composite.

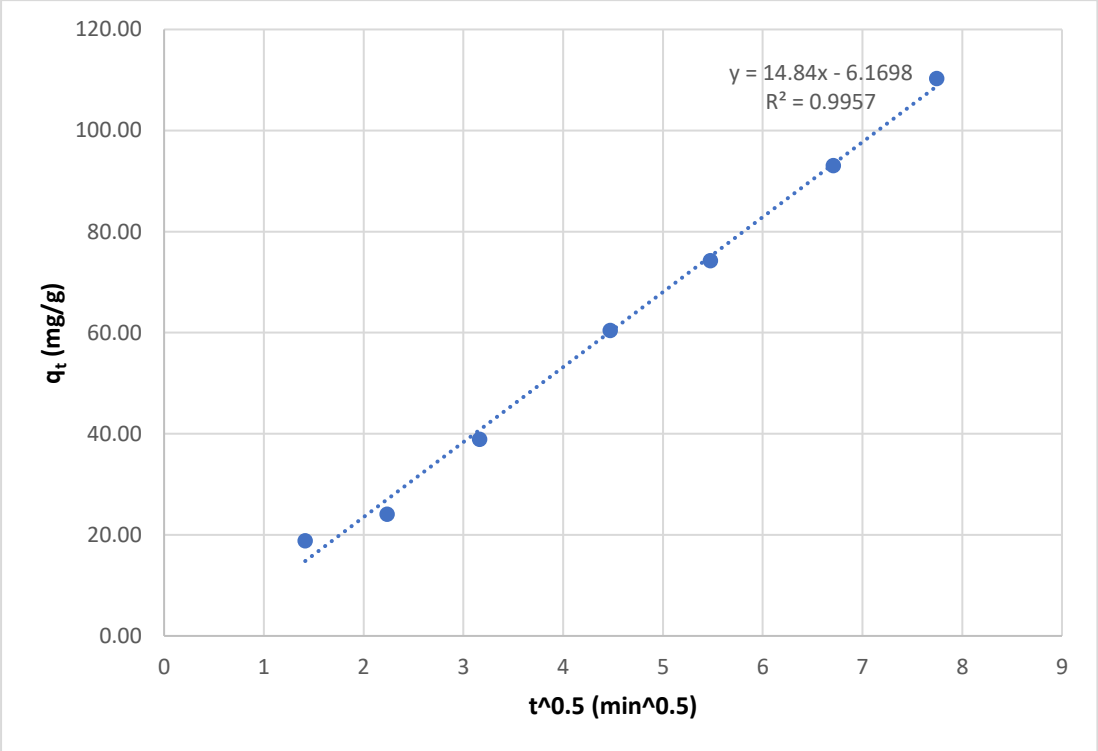

Fig. 35 The IPD investigation of INC sorption onto 5%V2O5@$MgAl_2O_4$ composite.

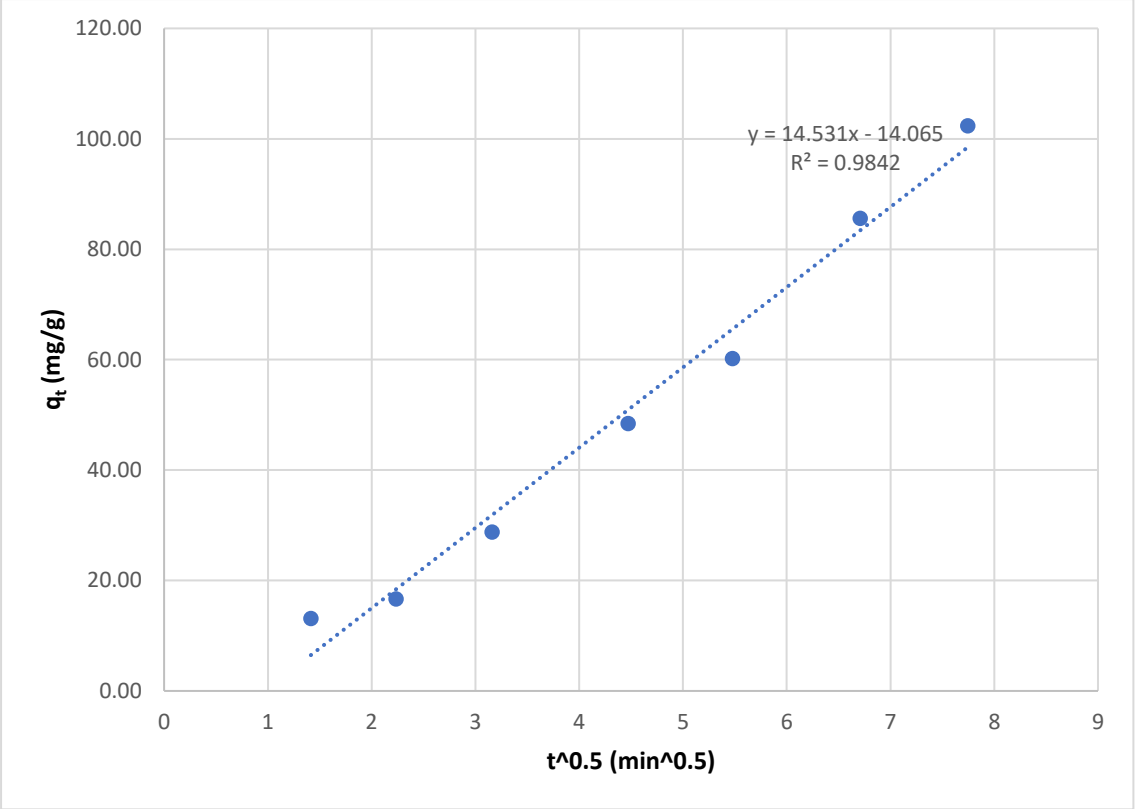

Fig. 36 The IPD investigation of INC sorption onto 10%V2O5@$MgAl_2O_4$ composite.

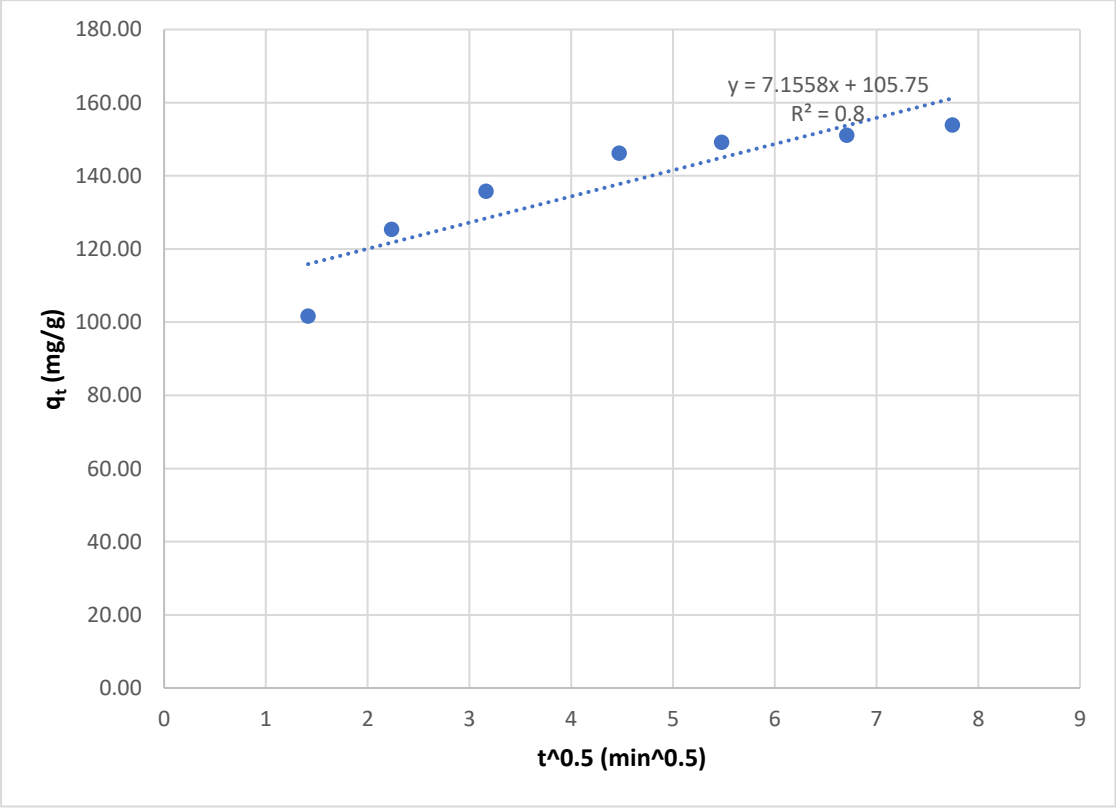

Fig. 37 The IPD investigation of BFC sorption onto $MgAl_2O_4$ composite

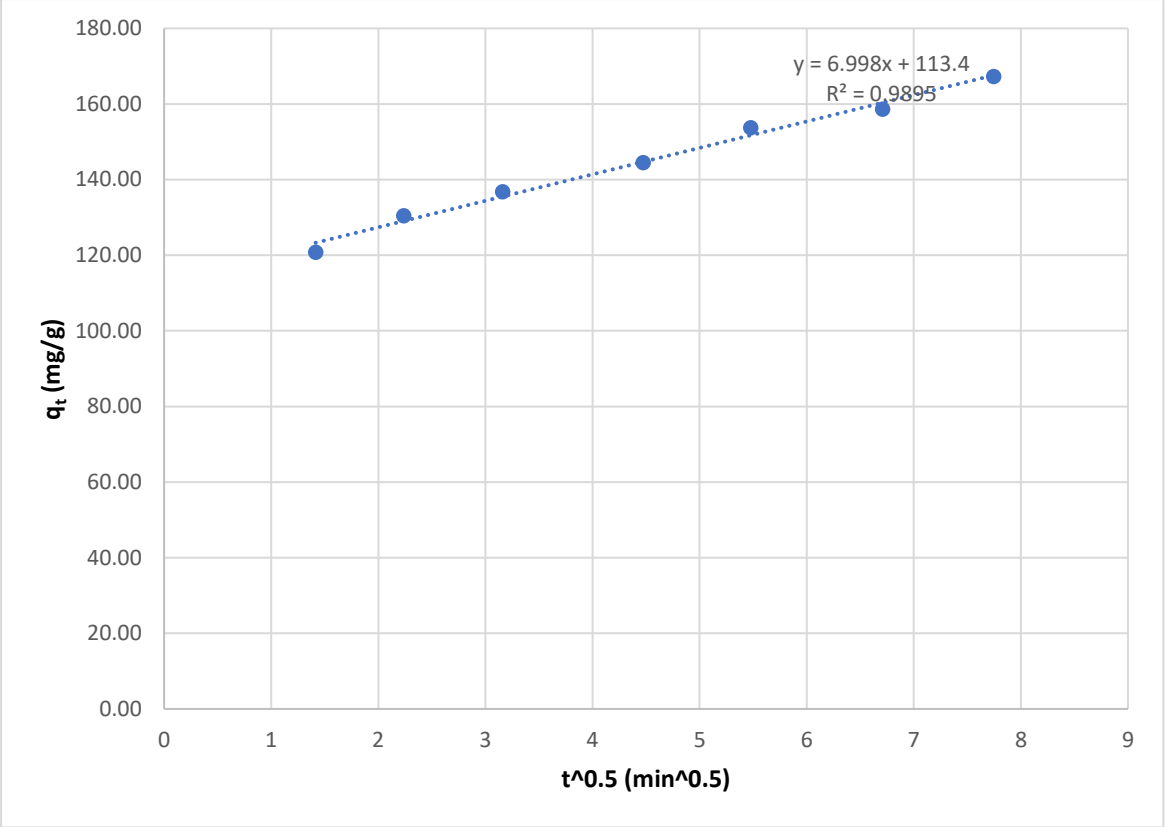

Fig. 38 The IPD investigation of BFC sorption onto 2.5%V2O5@$MgAl_2O_4$ composite.

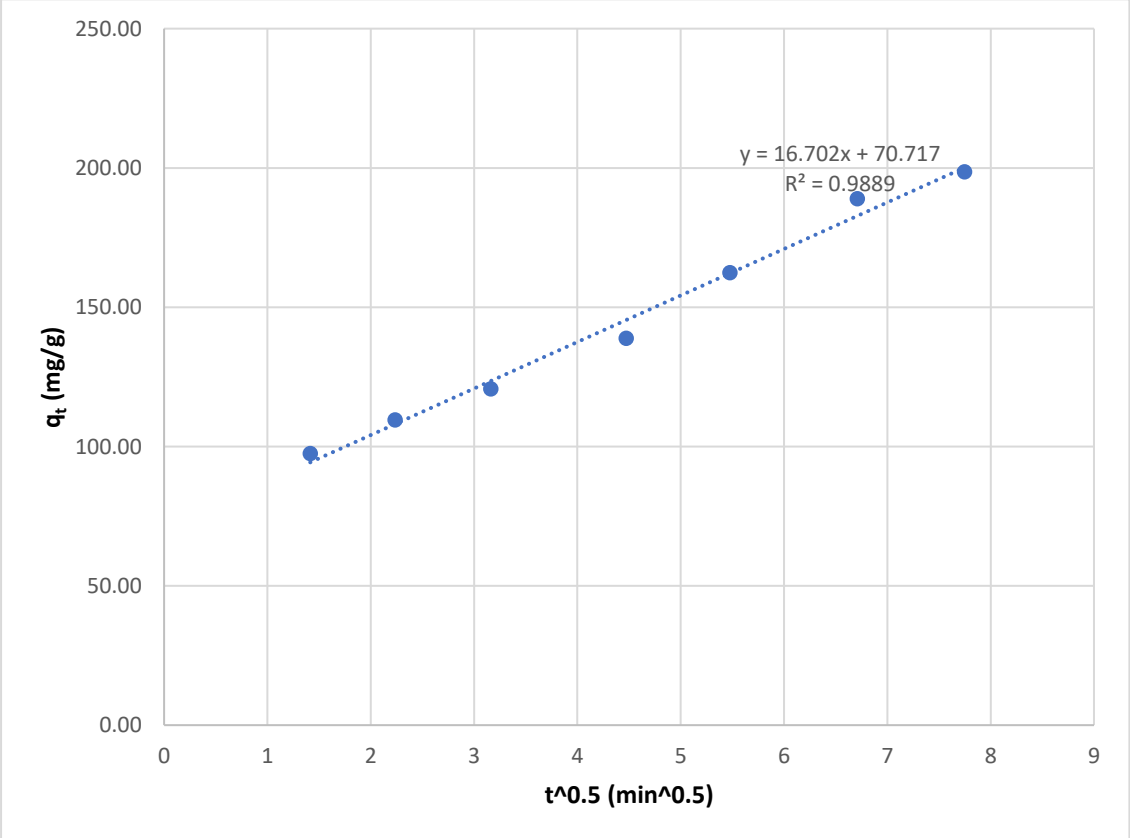

Fig. 39 The IPD investigation of BFC sorption onto 5%V2O5@$MgAl_2O_4$ composite.

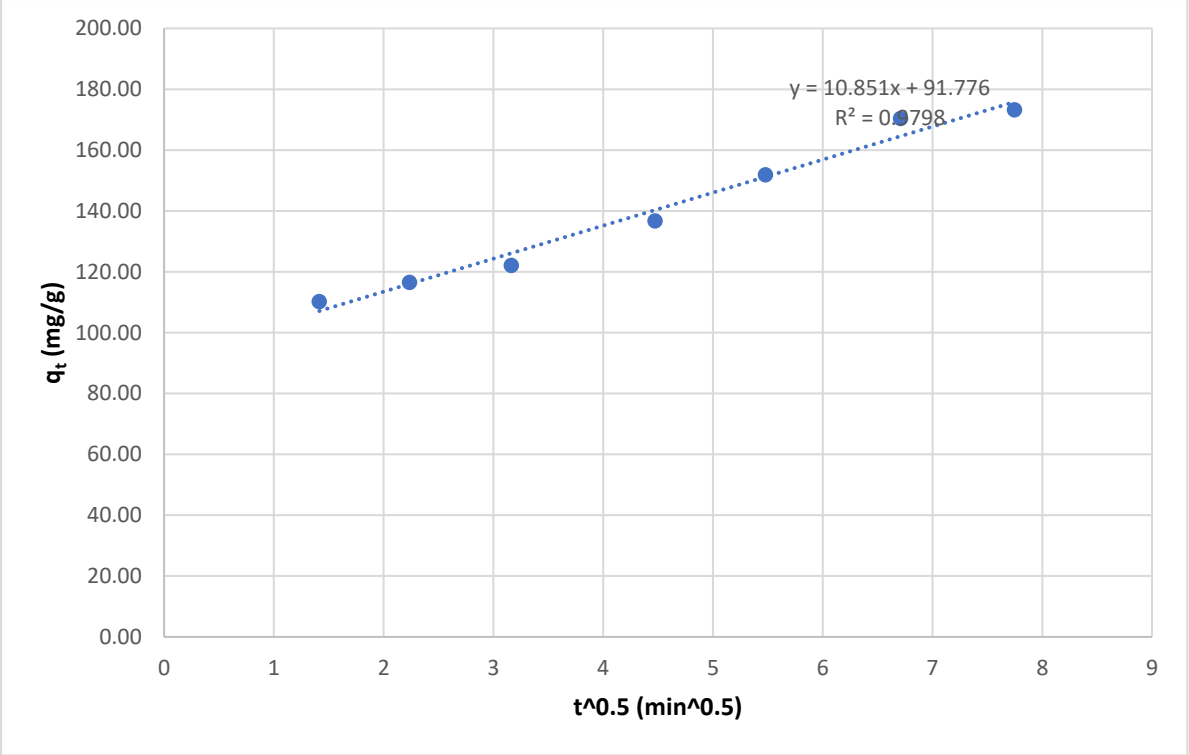

Fig. 40 The IPD investigation of BFC sorption onto 10%V2O5@$MgAl_2O_4$ composite.

Table 3 The adsorption rate control results of INC removal by $MgAl_2O_4$, 2.5%V2O5@$MgAl_2O_4$, 5%V2O5@$MgAl_2O_4$, and 10%V2O5@$MgAl_2O_4$.

Sorbent	*LFDM*		*IPDM*	
	K_{LF} (min^{-1})	R^2	K_{IP} (mg g^{-1} $min^{0.5}$)	R^2
AlMgO4	0.045	0.637	8.385	0.979
2.5%V2O5@$AlMgO_4$	0.039	0.992	10.054	0.995
5%V2O5@$AlMgO_4$	0.038	0.995	14.550	0.994
10%V2O5@$AlMgO_4$	0.037	0.991	13.798	0.979

Table 4 The adsorption rate control results of BFC removal by $MgAl_2O_4$, 2.5%V2O5@$MgAl_2O_4$, 5%V2O5@$MgAl_2O_4$, and 10%V2O5@$MgAl_2O_4$.

Sorbent	*LFDM*		*IPDM*	
	K_{LF} (min^{-1})	R^2	K_{IP} (mg g^{-1} $min^{0.5}$)	R^2
AlMgO4	0.076	0.952	7.156	0.800
2.5%V2O5@$AlMgO_4$	0.089	0.768	6.998	0.990
5%V2O5@$AlMgO_4$	0.105	0.800	16.702	0.989
10%V2O5@$AlMgO_4$	-0.079	0.933	10.851	0.980

3.4. Conclusion

This study used a fast method to prepare $MgAl_2O_4$, 2.5%V_2O_5@$MgAl_2O_4$, 5%V_2O_5@$MgAl_2O_4$, and 10%V_2O_5@$MgAl_2O_4$ composites. The synthesized composites were studied for removing INC and BFC from the water via adsorption. The $MgAl_2O_4$, 2.5%V2O5@$MgAl_2O_4$, 5%V2O5@$MgAl_2O_4$, and 10%V2O5@$MgAl_2O_4$ showed q_t values for INC were 75.91, 108.37, 147.30 and 118.54 mg g^{-1}, respectively, while for BFC they showed q_t values of 154.27, 167.38, 198.65 and 173.85 mg g^{-1}, respectively. The INC sorption reached its equilibrium at 90 minutes, while 60 minutes was sufficient for BFC sorption equilibration onto the four sorbents. The adsorption rate order of INC and BFC removal by $MgAl_2O_4$, 2.5%V2O5@$MgAl_2O_4$, 5%V2O5@$MgAl_2O_4$, and 10%V2O5@$MgAl_2O_4$ was studied via PF and PS kinetic models. The rate-order output of INC removals gathered in Table 1 illustrated that the sorption on four sorbents fitted the PS. Additionally, the BFC rate investigation output (Table 2) revealed the agreement of BFC sorption onto the $MgAl_2O_4$ and 2.5%V_2O_5@$MgAl_2O_4$ to the PF, while its sorpion onto 5%V_2O_5@$MgAl_2O_4$ and 10%V_2O_5@$MgAl_2O_4$ fitted the PF. Furthermore, The rate-control output of INC removal illustrated that the LFD controlled the sorption on 5%V_2O_5@$MgAl_2O_4$ and 10%V_2O_5@$MgAl_2O_4$, while IPD controlled it on $MgAl_2O_4$, and 2.5%V_2O_5@$MgAl_2O_4$. As for the BFC outputs, it revealed that IPD controlled the of BFC sorption onto all sorbent except of the $MgAl_2O_4$.

References

1. Hasan, S.J.R.J.R.S., *A review on nanoparticles: their synthesis and types.* 2015. **2277**: p. 2502.
2. Rajput, N., *Methods of preparation of nanoparticles-a review.* International Journal of Advances in Engineering & Technology, 2015. **7**(6): p. 1806.
3. Duong, V.-A., T.-T.-L. Nguyen, and H.-J. Maeng, *Preparation of Solid Lipid Nanoparticles and Nanostructured Lipid Carriers for Drug Delivery and the Effects of Preparation Parameters of Solvent Injection Method.* Molecules, 2020. **25**(20): p. 4781.
4. Tissue, B. and H.J.J.o.S.S.C. Yuan, *Structure, particle size, and annealing of gas phase-condensed Eu3+: Y2O3 nanophosphors.* 2003. **171**(1-2): p. 12-18.
5. Hasany, S., et al., *Systematic review of the preparation techniques of iron oxide magnetic nanoparticles.* 2012. **2**(6): p. 148-158.
6. Arole, V. and S.J.J.M.S. Munde, *Fabrication of nanomaterials by top-down and bottom-up approaches-an overview.* 2014. **1**: p. 89-93.
7. Houshiar, M., et al., *Synthesis of cobalt ferrite (CoFe2O4) nanoparticles using combustion, coprecipitation, and precipitation methods: A comparison study of size, structural, and magnetic properties.* 2014. **371**: p. 43-48.
8. Minemoto, T., et al., *Preparation of Zn1− xMgxO films by radio frequency magnetron sputtering.* 2000. **372**(1-2): p. 173-176.
9. Tadic, M., et al., *Magnetic properties of novel superparamagnetic iron oxide nanoclusters and their peculiarity under annealing treatment.* 2014. **322**: p. 255-264.
10. Sun, C., et al., *Versatile application of a modern scanning electron microscope for materials characterization.* 2020. **55**(28): p. 13824-13835.
11. Sadiq, I.M., et al., *Antimicrobial sensitivity of Escherichia coli to alumina nanoparticles.* 2009. **5**(3): p. 282-286.
12. Tyner, K.M., S.R. Schiffman, and E.P.J.J.o.C.R. Giannelis, *Nanobiohybrids as delivery vehicles for camptothecin.* 2004. **95**(3): p. 501-514.
13. Sun, P., et al., *Aluminium-induced inhibition of root elongation in Arabidopsis is mediated by ethylene and auxin.* 2010. **61**(2): p. 347-356.
14. Pachiyappan, J., et al., *Preparation and characterization of magnesium oxide nanoparticles and its application for photocatalytic removal of rhodamine B and methylene blue dyes.* 2022. **2022**.
15. Xu, L., H. Song, and L.J.A.C.B.E. Chou, *Carbon dioxide reforming of methane over ordered mesoporous NiO–MgO–Al2O3 composite oxides.* 2011. **108**: p. 177-190.
16. Li, Y., et al., *Pyrolysis and catalytic upgrading of low-rank coal using a NiO/MgO–Al2O3 catalyst.* 2016. **155**: p. 194-200.
17. Sallal, H.A., et al., *Preparation of Al2O3/MgO Nano-Composite Particles for Bio-Applications.* 2020. **38**(4): p. 586-593.
18. Biswas, P., C.-Y.J.J.o.t.a. Wu, and w.m. association, *Nanoparticles and the environment.* 2005. **55**(6): p. 708-746.
19. Madhav, S., et al., *Water pollutants: sources and impact on the environment and human health.* Sensors in water pollutants monitoring: Role of material, 2020: p. 43-62.
20. MISHRA, R., et al., *INVESTIGATION OVER WATER QUALITY OF RIVERS GANGA AND YAMUNA DURING KUMBH-2019-A CASE STUDY AT PRAYAGRAJ (ALLAHABAD), UTTAR PRADESH, INDIA.*
21. Yihdego, Z.J.B.R.P.i.I.W.L., *The fairness 'dilemma'in sharing the Nile waters: what lessons from the grand Ethiopian renaissance dam for international law?* 2017. **2**(2): p. 1-80.
22. Manahan, S., *Environmental chemistry*. 2017: CRC press.
23. Verma, J., et al., *Marine pollution, sources, effect and management.* Three Major Dimensions of Life: Environment, Agriculture and Health. Prayagraj, India: Society of Biological Sciences and Rural Development, 2020: p. 270-276.

24. Shumiye, W.B., et al., *Exergy analysis of solar-geothermal based power plant integrated with boiling, and reverse osmosis water purification.* Energy Conversion and Management: X, 2022. **15**: p. 100255.
25. Shannon, M.A., et al., *Science and technology for water purification in the coming decades.* Nature, 2008. **452**(7185): p. 301-310.
26. Jiménez, S., et al., *Produced water treatment by advanced oxidation processes.* Science of the Total Environment, 2019. **666**: p. 12-21.
27. You, W., K.J. Noonan, and G.W. Coates, *Alkaline-stable anion exchange membranes: A review of synthetic approaches.* Progress in Polymer Science, 2020. **100**: p. 101177.
28. Qasem, N.A., R.H. Mohammed, and D.U. Lawal, *Removal of heavy metal ions from wastewater: A comprehensive and critical review.* Npj Clean Water, 2021. **4**(1): p. 36.
29. Calvet, R., *Adsorption of organic chemicals in soils.* Environmental health perspectives, 1989. **83**: p. 145-177.
30. Moreno-Castilla, C., *Adsorption of organic molecules from aqueous solutions on carbon materials.* Carbon, 2004. **42**(1): p. 83-94.